



Cite this: *Sustainable Energy Fuels*,  
2026, 10, 1382

# Humidity-driven energy harvesting systems: mechanisms, materials, challenges, and future directions

Soheil Malekghasemi <sup>\*ac</sup> and Serdar Abaci <sup>\*b</sup>

The continuous advancement in low-power electronics, wearable devices, and autonomous sensing platforms has increased the demand for energy harvesting technologies capable of extracting power from ambient energy sources. Among these sources, atmospheric humidity has recently emerged as a promising source for micro-scale power generation, as ambient moisture gradients can drive ion transport in hygroscopic materials to produce electrical output for low-power electronics and self-powered sensors. Recently, the systems like moisture-enabled electric generators (MEGs), hygroelectric converters, and evaporation-induced energy harvesters have shown the capability to transform water vapor or humidity gradients into usable electrical energy, utilizing environmentally friendly materials and *via* passive operation. This review presents a comprehensive overview of the fundamental mechanisms, materials, and device architectures that define humidity-driven energy harvesting technologies. Current methods are categorized according to their operational principles, such as ionic diffusion, surface charge modulation, and evaporation-driven flow. Key material systems, including carbon-based films, hydrogels, metal oxides, and bio-inspired composites, are examined for their performance, durability, and scalability. The discussion also includes the integration of these harvesting systems with energy storage components as a means to achieve fully autonomous and self-sufficient power platforms. This review focuses on applications in wearable technology, environmental monitoring, and the Internet of Things (IoT) to emphasize the potential impact of humidity-powered systems in practical situations. Finally, the current limitations in power output, environmental sensitivity, and fabrication complexity are critically examined, and future research directions are suggested. This review aims to summarize emerging knowledge in this field and promote the advancement of next-generation humidity-enabled energy technologies for decentralized and sustainable energies.

Received 7th October 2025  
Accepted 27th January 2026

DOI: 10.1039/d5se01325a

rsc.li/sustainable-energy

## 1. Introduction

The shift towards sustainable energy systems represents a significant scientific and technological challenge of the 21st century.<sup>1</sup> The increasing prevalence of mobile, wearable, and embedded electronic systems, particularly within healthcare, environmental monitoring, and the internet of things (IoT), has created a critical need for micro-scale energy solutions that are autonomous and environmentally friendly.<sup>2,3</sup> These emerging applications frequently function in areas where conventional power sources, such as batteries or grid connections, are unfeasible, short-lived, or environmentally unsustainable.<sup>4,5</sup> As a result, researchers are increasingly focusing on ambient

energy harvesting strategies that exploit natural energy flows present in the environment, such as light, heat, mechanical vibrations, and humidity.<sup>6</sup>

Despite considerable scientific progress in solar, thermo-electric, and piezoelectric energy harvesters, each has its distinct limitations. Photovoltaics demonstrate remarkable efficiency when exposed to optimal lighting conditions, but they encounter challenges due to poor performance in indoor settings, intermittent availability, and vulnerability to environmental deterioration.<sup>7</sup> Thermoelectric generators require a temperature gradient to operate efficiently, limiting their use to specific applications such as industrial waste heat recovery.<sup>8</sup> Similarly, piezoelectric and triboelectric systems rely on dynamic mechanical motion and are often unsuitable for stationary or passive situations.<sup>9</sup> These limitations underscore the necessity to investigate alternative ambient energy sources that are more prevalent and more aligned with the requirements of low-power and distributed electronics.

Atmospheric moisture, a stable and abundant feature of terrestrial environments, offers a relatively unknown but

<sup>a</sup>Department of Bioengineering, Graduate School of Science and Engineering, Hacettepe University, 06800 Beytepe, Ankara, Türkiye. E-mail: soheil.mgh@gmail.com

<sup>b</sup>Department of Chemistry, Hacettepe University, 06800 Beytepe, Ankara, Türkiye. E-mail: sabaci@hacettepe.edu.tr

<sup>c</sup>ICET Enerji Inc., Innovative Clean Energy Technologies, Bilkent Cyberpark, 06450, Ankara, Türkiye



promising source of environmental energy.<sup>10</sup> The Earth's atmosphere holds a considerable amount of water vapor, averaging about 12 900 cubic kilometers globally, which corresponds to roughly 0.001% of the planet's total water volume. Interactions with functional materials can induce electrochemical and electrostatic phenomena, which may be harnessed for electricity generation.<sup>11,12</sup> Humidity exists in both outdoor and indoor settings, encompassing shaded, enclosed, or otherwise hard-to-reach areas where solar or thermal gradients are inadequate.<sup>13,14</sup> This makes humidity-driven energy harvesting particularly suitable for powering distributed sensor networks, low-power embedded systems, and other off-grid technologies.

The origins of humidity-to-electricity conversion are traced back to early electrostatic observations. In 1840, Lord William Armstrong first elucidated a phenomenon in which steam jets released from a boiler produced a significant electrostatic charge, henceforth referred to as the Armstrong Effect.<sup>15</sup> Systematic studies into this effect were carried out by Michael Faraday in 1843.<sup>16</sup> He ascribed the electrification to the friction between metal surfaces and condensed water droplets, which allowed for the transfer of ions and the charging of the surfaces. Foundational insights into moisture-induced charge generation have established the basis for current humidity energy research. Currently, advanced materials, including graphene oxide membranes, hygroscopic polymers, and bioinspired films, utilize humidity gradients and vapor absorption to generate electricity efficiently. Recent improvements in nanomaterial engineering and thin-film fabrication have enabled the precise regulation of surface wettability, ion mobility, and charge separation, thus enhancing the effectiveness and applicability of humidity-driven energy systems.

Between the early electrostatic observations of the 19th century and the recent proliferation of moisture-powered technologies, foundational theoretical and experimental studies have laid crucial groundwork. In 2004, Bazant and Squires presented the concept of induced-charge electrokinetic phenomena, demonstrating that nonlinear flows adjacent to polarized surfaces can result in streaming currents and electrokinetic pumping when subjected to weak electric fields.<sup>17</sup> In 2010, Bocquet and Charlaix synthesized advances in nanofluidics, focusing on confined water transport and electrokinetic coupling at solid-liquid interfaces.<sup>18</sup> In 2012, Jouniaux and Bordes conducted a review of frequency-dependent streaming potentials in porous media, thereby expanding the theoretical foundation for electrokinetic energy conversion.<sup>19</sup> On the materials side, Ghosh and co-workers in 2003 demonstrated that ionic fluid flow through carbon nanotubes generated measurable electrical signals, providing one of the earliest indications that nanostructured channels could convert fluid motion into electricity.<sup>20</sup> This was followed by Jung and co-workers in 2008, who documented how exposure to water vapor significantly alters the electrical conductivity of reduced graphene oxide (rGO) sheets, with behavior explainable through adsorption kinetics. They explicitly mention that these changes are relevant for gas sensor applications.<sup>21</sup> In 2015, Zhao *et al.* demonstrated that moisture adsorption on graphene oxide

layers could generate sustained voltage outputs.<sup>22</sup> In 2017, this finding was further clarified by Chang and Baek in their study of charge transport mechanisms in graphene oxide.<sup>23</sup> In 2017, it was revealed that porous carbon-black sheets produce continuous voltage when subjected to evaporative flux, representing a significant advancement in the development of hydrovoltaic devices.<sup>24</sup> In 2018, the term “hydrovoltaic effect” was officially created to characterize electricity production resulting from the interaction of water with nanostructured materials, therefore consolidating this emerging field under a unifying concept.<sup>25</sup> Together, these studies from the early 2000s to the late 2010s formed the bridge between theoretical electrokinetics and application-oriented humidity-harvesting systems, which have rapidly expanded since 2022.

In recent years, a number of technologies have emerged that can convert moisture into usable electrical energy. These include moisture-enabled electric generators (MEGs), hygroelectric generators, and evaporation-driven energy harvesters.<sup>26–28</sup> Although the mechanisms vary among these systems, they are generally based on ion diffusion, surface charge modulation, or evaporation flow through asymmetric material structures.<sup>29,30</sup> These systems are generally fabricated from lightweight, low-cost, and often biodegradable materials, including carbon-based films, hydrogels, or metal oxides. Although these technologies are relatively new, they have demonstrated the capability to produce continuous albeit low-power, electrical outputs that are appropriate for powering microscale devices.<sup>31–33</sup>

However, the progress of humidity-driven energy harvesting systems is still in its initial phases. Many prototypes continue to be restricted to laboratory-scale demonstrations, exhibiting limited long-term stability, low energy conversion efficiency, and narrow environmental adaptability. Additionally, the lack of standard methods and benchmarking protocols makes it difficult to compare device performance across studies.<sup>34</sup> Finally, several current systems function exclusively as energy harvesters and do not possess energy storage capabilities, limiting their effectiveness for practical applications that require a reliable power supply.<sup>35</sup>

The growing interest in moisture-powered systems is also reflected in emerging interdisciplinary research efforts that integrate principles from materials science, surface chemistry, electrokinetics, device engineering, and system design. A distinct trend is emerging in the design of multifunctional platforms that incorporate energy harvesting with additional functionalities, including sensing, actuation, and wireless data transmission.<sup>36–38</sup> As the field continues to evolve, innovative device designs are anticipated to provide superior energy output with enhancements in mechanical flexibility, form factor, environmental durability, and overall system integration. The long-term vision encompasses the seamless integration of humidity-responsive components into smart textiles, construction materials, and implantable devices, with an emphasis on compactness and energy autonomy as critical factors.<sup>39,40</sup>

This review aims to provide a comprehensive and insightful overview of the present landscape of humidity-driven energy harvesting technologies. This review begins by classifying and



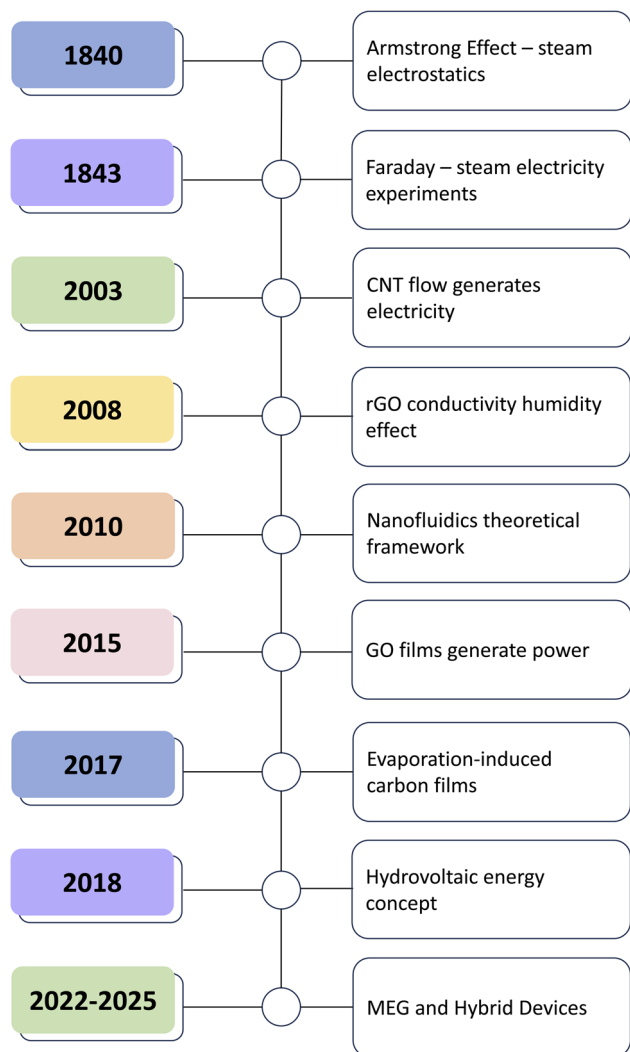


**Fig. 1** Key milestones in the evolution of humidity-to-electricity conversion: In 1840, Armstrong described the discovery of electrostatic charge from steam jets.<sup>15</sup> In 1843, Faraday's experiments showed steam-driven electricity.<sup>16</sup> In 2003, electrical signals were detected from ionic fluid flow through carbon nanotubes.<sup>20</sup> In 2008, reduced graphene oxide sheets were shown to exhibit humidity-dependent conductivity.<sup>21</sup> In 2010, theoretical advances in nanofluidics clarified confined water transport and electrokinetic coupling.<sup>18</sup> In 2015, graphene oxide films were demonstrated to generate direct power from moisture exposure.<sup>22</sup> In 2017, evaporation-induced electricity was achieved in nanostructured carbon films.<sup>24</sup> In 2018, the concept of hydrovoltaic energy was formalized,<sup>25</sup> and since 2022, rapid progress has been made in moisture-enabled generators, hybrid devices, and integrated storage systems.<sup>17,172</sup>

elucidating the core principles that underpin various approaches to moisture-enabled electricity generation. The focus then shifts to the material systems employed in device construction, emphasizing their significance in efficiency, stability, and scalability. The integration of energy storage components into humidity-harvesting devices is subsequently discussed, highlighting their significance for fully autonomous systems. This review ultimately delves into significant applications, highlights existing limitations, and presents future

research avenues that may expedite the advancement of next-generation self-powered systems.

This review provides a resource for scientists and engineers involved in the development of sustainable, compact, humidity-driven energy solutions for practical applications. This approach consolidates multiple research strands into a cohesive framework that fosters innovation in the field of study.

The advancement of humidity-driven energy harvesting has markedly progressed over the last two centuries, transitioning from fundamental electrostatic findings to contemporary innovations in hybrid nanogenerators. A visual timeline of key milestones (Fig. 1) showcases the significant advances that have influenced the field, encompassing the discovery of graphene oxide's humidity sensitivity, evaporation-driven processes, wearable MEG systems, and hybrid devices with integrated storage and communication capabilities.

## 2. Classification of humidity-driven energy conversion mechanisms

Energy harvesting technologies driven by humidity can be broadly categorized according to their fundamental physical mechanisms. Although all systems depend on atmospheric moisture as an energy source, the approach to extracting electrical energy differs considerably among the various designs. The variations originate from the materials employed, device configurations, and the specific interactions occurring between water molecules and functional surfaces. This section categorizes humidity-based energy harvesting systems into four main classes: (i) ionic diffusion and electrokinetic systems, (ii) surface charge and hygroelectric effect-based systems, (iii) evaporation-induced flow generators, and (iv) triboelectric generators influenced by humidity. Each mechanism is examined with a focus on the physical principles, representative materials, and performance characteristics. To provide a clear visual comparison, Fig. 2 illustrates the four primary humidity-driven electricity generation mechanisms. Each approach reflects a distinct interaction pathway between water molecules and functional surfaces, and collectively, they underpin the diversity of moisture-enabled energy technologies.

It should be noted that the terminology in humidity-driven energy harvesting literature has not yet been standardized. Terms such as “moisture-enabled electric generator,” “hygroelectric generator,” and “humidity-driven energy harvester” are often used interchangeably, even when distinct physical mechanisms are involved. In this review, classification is therefore based strictly on the dominant energy conversion mechanism rather than on the terminology adopted in the original publications. In particular, systems relying on bulk ionic diffusion, proton transport, or electrochemical concentration gradients are distinguished from those governed primarily by surface charge redistribution or dipole-induced potential modulation. Transitional and hybrid cases are discussed explicitly, where appropriate.



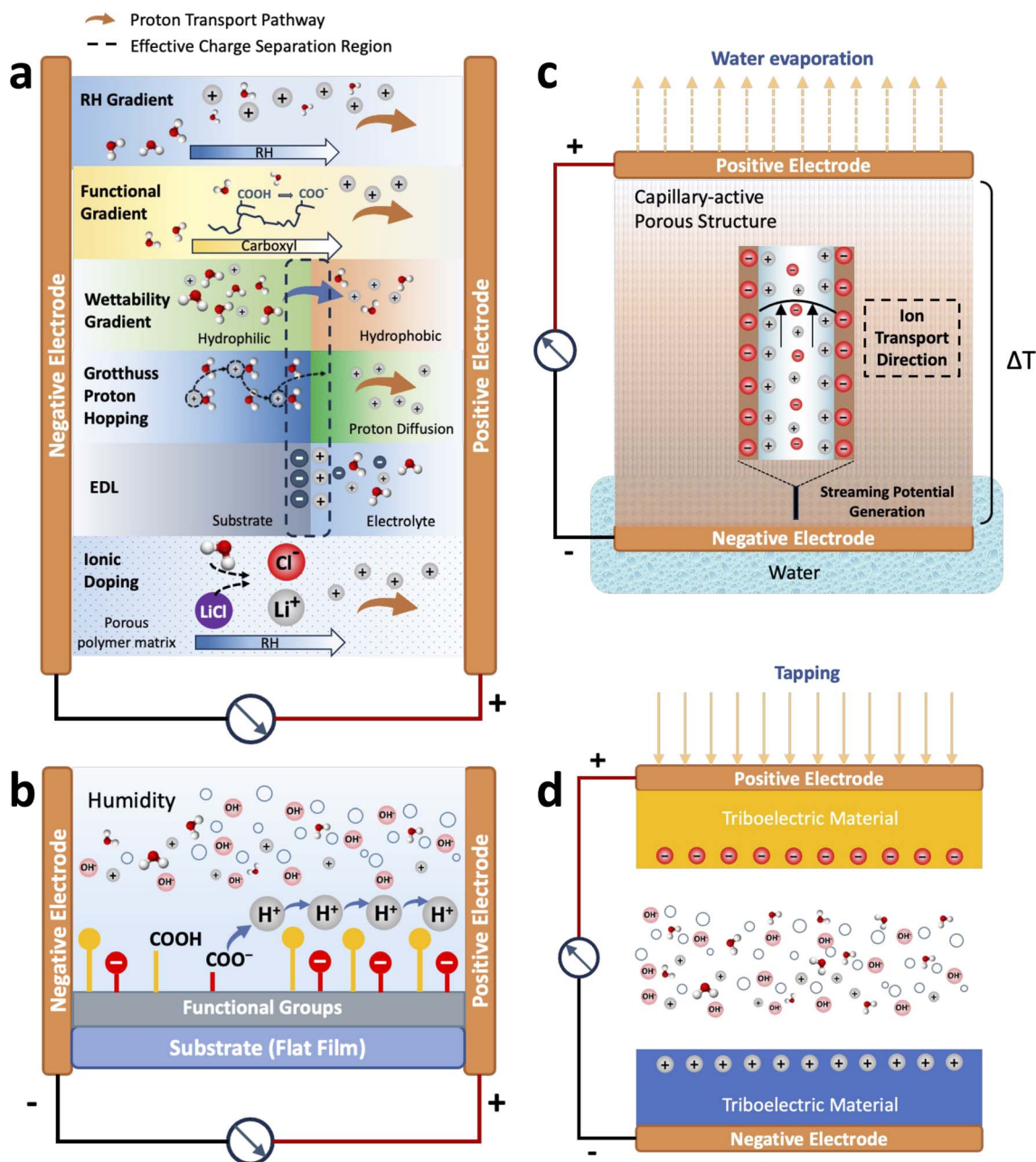


Fig. 2 Schematic of the four primary mechanisms of humidity-driven electricity generation. (a) Ionic diffusion and electrokinetic systems utilize humidity-induced concentration gradients in hygroscopic media to drive ion migration and generate voltage. Key driving forces include asymmetric humidity exposure, gradients in surface functional groups, wettability-induced moisture distribution, and built-in electrostatic fields. Enhanced transport is further supported by the Grotthuss-type proton hopping, electric double layer formation, and ionic composite doping, collectively enabling efficient charge flow and voltage generation. (b) Surface charge modulation (hygroelectric effect) arises from water adsorption on polar or semiconducting surfaces, altering surface potential and inducing dipoles. (c) Evaporation-induced streaming and thermodiffusion-based systems convert capillary flow and evaporation into electric signals through streaming potentials and temperature gradients. (d) TENGs are modulated by ambient humidity, which influences surface charge retention and electrostatic interactions during contact-separation cycles. These diverse mechanisms underpin the versatility of moisture-enabled energy harvesting platforms.

### 2.1 Ionic diffusion and electrokinetic systems

Among the most researched humidity-based energy harvesting systems are those that rely on bulk ionic transport processes, primarily ion diffusion driven by concentration gradients and/or the formation of electric double layers (EDL), and phenomena that take place when hygroscopic materials come

into contact with atmospheric moisture. In this review, such systems are classified based on their dominant electrochemical and electrokinetic mechanisms regardless of whether they are labeled as “moisture-enabled electric generators” or “hygroelectric devices” in the original literature. These systems harness electrical energy when water molecules are absorbed by



materials that contain functional groups like hydroxyl (–OH), carboxyl (–COOH), or sulfonic acid (–SO<sub>3</sub>H). Upon exposure to humidity, these functional groups dissociate, releasing mobile cations, mainly protons, which act as charge carriers.<sup>41–43</sup>

The presence of a concentration gradient of these ions across the material triggers the ions to migrate in a direction, which in turn creates an internal electrochemical potential difference and produces a voltage between the two electrodes.

This process is referred to as gradient diffusion and can be initiated through two main strategies. The first involves asymmetric exposure to moisture, for instance, by positioning one side of the device in a high-humidity environment while keeping the other side under drier conditions. This results in a localized rise in ion concentration on one side, leading to the generation of a net diffusion current (Fig. 2a).<sup>43,44</sup> The second strategy is based on the structural asymmetry of surface functional groups. In this context, areas with a higher density of dissociable sites tend to release more ions when moisture is absorbed, which facilitates the movement of ions toward regions with fewer functional groups (Fig. 2a).<sup>45</sup>

In many reported devices, these processes are electrochemically analogous to moisture-activated concentration cells, where humidity regulates ionic activity and electrode potentials rather than inducing purely electronic surface polarization. This mechanism systematically converts the chemical potential energy of adsorbed water molecules into electricity. Protons often play a key role in this diffusion process, and their mobility greatly affects the resulting electrical output. Improving performance relies on optimizing the surface chemistry, boosting the density and polarity of functional groups, and engineering the material geometry to promote sustained concentration gradients.

In some cases, a hydrophilic-hydrophobic gradient is created along the length of the material to enhance directional ion flow (Fig. 2a).<sup>46</sup> This gradient encourages asymmetric water absorption, resulting in improved ionic movement and stronger concentration gradients. Polymeric systems, carbon-based materials, and metal oxides, particularly when combined with ionic electrolytes or surface-active salts, have been utilized to enhance ionic conductivity and boost charge separation efficiency *via* humidity-activated ion transport mechanisms (Fig. 2a).<sup>43,47,48</sup> These composite designs expand the range of materials that can be utilized and provide flexibility in both structure and performance.

Materials frequently used in these systems include graphene oxide, cellulose-based films, carbon nanotubes, conducting polymers, and metal oxide frameworks.<sup>22,46,49–52</sup> GO–ZnO heterostructures, for instance, have demonstrated humidity-driven voltage generation *via* proton-hopping transport facilitated by adsorbed water molecules. This transport process is well-explained by the Grotthuss mechanism, in which protons rapidly transfer along a hydrogen-bonded water network, enhancing electrokinetic output through continuous ion migration across functional surfaces (Fig. 2a).<sup>53</sup> Basically, this process can be viewed as protons ‘passing along’ a chain of water molecules rather than physically flowing across the entire substance. As water molecules continuously form and break

hydrogen bonds, the charge is transferred efficiently through the network, allowing for electrical generation even with modest bulk ion movement. Although open-circuit voltages of several volts have been reported, the current density and power output remain relatively modest, reflecting limitations in sustained ion flux. Nevertheless, the straight-forward nature, environmental compatibility, and scalability of these systems make them attractive for autonomous micro-energy and sensing applications.

Beyond bulk ionic diffusion and proton hopping, recent work has revealed that interfacial ion–electron conversion can play a decisive role in enhancing moisture-enabled electricity generation. A recent study demonstrated that rationally engineered ion–electron conversion interfaces enable efficient transduction of humidity-driven ionic flux into electronic current, considerably improving power output and stability. This mechanism bridges electrochemical ion transport and electronic conduction, offering a new design paradigm for next-generation MEGs with improved efficiency and interfacial robustness.<sup>54</sup>

Overall, these systems operate through a range of interrelated mechanisms, including asymmetric humidity exposure, surface chemical gradients, wettability-induced moisture gradients, Grotthuss-type proton hopping, electrolyte-enhanced conductivity, and bilayer electrostatic structures, all unified by the fundamental principle of humidity-driven directional ionic migration within the bulk or near-surface regions of functional materials.

## 2.2 Surface charge modulation and hygroelectric effect-based systems

A distinct class of humidity-driven energy conversion mechanisms is based on surface-dominated charge modulation processes in which electrical output arises primarily from changes in surface potential induced by water molecule adsorption. This phenomenon, commonly known as the hygroelectric effect, which in this review is defined narrowly as voltage generation dominated by surface charge redistribution or dipole-induced potential modulation rather than bulk ionic diffusion (Fig. 2b).<sup>55,56</sup>

Unlike gradient diffusion systems, which rely on ion transport across a bulk material, surface charge modulation mechanisms operate mainly at the interface between the material and the surrounding atmosphere. Polar water molecules interact with surface functional groups, modifying the electronic structure and consequently influencing the surface work function or inducing charge polarization. This results in the development of a measurable voltage difference across the material.

Semiconductor and dielectric materials, such as ZnO, TiO<sub>2</sub>, graphitic carbon nitride (g-C<sub>3</sub>N<sub>4</sub>) and various biomolecular films, have presented potential in hygroelectric systems. Transparent and flexible ZnO nanofilms have proven their capacity to produce a stable and measurable electric output by exploiting moisture-induced surface charge modulation, even in the presence of mechanical deformation and fluctuating







**Table 1** Comparison of humidity-driven energy harvesting mechanisms

Mechanism	Primary principle	Representative material systems	Typical output characteristics	Advantages	Challenges	Typical applications	Ref
Ionic diffusion and electrokinetic (MEGs)	Directional ion migration driven by concentration gradients, surface functional group asymmetry, or hydrophilic-hydrophobic gradients; may involve Grotthuss proton hopping	GO, GO-ZnO heterostructures, cellulose nanofibers, polyelectrolytes (e.g., PDDA:PSS), conducting polymers, metal oxides	Voltage: 0.5–3 V; current: $\mu\text{A}$ to mA range; power density: $\mu\text{W}$ to $\text{mW cm}^{-2}$ depending on geometry	Simple, scalable, environmentally benign, continuous DC output under humidity gradient	Low power density; requires sustained RH difference; limited current	Autonomous IoT nodes, environmental sensors, flexible/wearable electronics	41–52
Surface charge modulation (hygroelectric)	Water molecule adsorption alters surface potential/work function <i>via</i> dipole induction and charge redistribution	ZnO nanofilms, $\text{TiO}_2/\text{g-C}_3\text{N}_4$ composites, $\text{WO}_3$ nanowires, bio-nano hybrids (e.g., Geobacter- $\text{CN}_2$ ), protein films, graphene-based films	Voltage: tens-hundreds of mV; response time: 30 ms to 2 s; power density: up to $\sim 123 \text{ mW m}^{-2}$ (with hybrid PV coupling)	Fast response, interface-based, reversible operation, no moving parts	Low output power; environmental instability; surface contamination sensitivity	Humidity sensors, self-powered triggers, bio-integrated devices	55–65
Evaporation-induced flow/thermodiffusion	Capillary-driven water transport and evaporation create streaming potentials, pressure gradients, or thermal gradients (evapoelectrics)	Porous $\text{Al}_2\text{O}_3$ membranes, carbonized PAN nanofibers, LiCl-loaded hydrogels, layered hydrogel-AAO composites, cellulose membranes	Voltage: 0.1–0.65 V; current: $\mu\text{A}$ range; power density: up to $>1 \text{ W m}^{-2}$ (evapoelectrics)	Continuous operation in humid/outdoor settings, biologically inspired	Requires a sustained water supply; performance declines in dry conditions	Outdoor environmental sensors, low-power autonomous devices	28,66–72
Triboelectric nanogenerators (TENGs)	Contact electrification and electrostatic induction between materials; humidity influences charge transfer and retention	Polymers (PTFE, Ecoflex), PVA/LiCl-MXene composites, GO-GONR films, MOF-polymer hybrids, CNT-hydrogel electrodes	Voltage: up to 300 V; current: $\mu\text{A}$ range; power density: tens of $\text{mW m}^{-2}$ ; response: $<1 \text{ s}$	High peak voltage, flexible formats, hybrid integration with MEG possible	Output strongly affected by humidity; charge loss at high RH; complex optimization	Wearable motion sensors, humidity-adaptive electronics, hybrid energy harvesters	73–80

moisture interferes with surface charge transfer during contact-separation cycles. The presence of moisture in the atmosphere adversely impacts charge transfer, resulting in a progressive decrease in the amount of charge transferred as humidity levels rise. Moreover, humidity alters the physical and dielectric properties of natural or synthetic textile materials, which is reflected in the decline in electric output when these materials are used as triboelectric layers. In contrast, composite TENGs that incorporate hygroscopic materials like LiCl and two-dimensional transition metal carbides, nitrides, and carbonitrides (MXene) can enhance their output three times under conditions of high relative humidity, demonstrating the dual impact of moisture on triboelectric performance.<sup>75</sup> This improvement is due to the rich hydroxyl groups in PVA, the significant hygroscopic properties of LiCl, and the micro-capacitor network formed by MXene nanosheets. Together, these features enhance the water absorption capacity and surface roughness, resulting in improved triboelectric performance.

Furthermore, recent research has shown that graphene oxide nanoribbons (GONRs) can markedly improve the self-powered humidity sensing performance of GO-based TENGs.<sup>76</sup> Paper-based TENGs fabricated with GO, GO + GONR, and GONR/GO configurations achieved maximum voltage outputs above 300 V, with voltage response enhancements of up to 124%. The rapid response (0.3 s) and recovery (0.5 s) characteristics were ascribed to the elevated density of oxygenated functional groups and edge defects in GONRs, which enhanced the diffusion of bulk water molecules. This strategy shows promise for advanced humidity-responsive TENG designs that are useful in both sensing and energy applications.

Humidity affects the dielectric properties, surface conductivity, and charge retention of triboelectric materials. Increased moisture generally leads to enhanced surface conductivity and dielectric breakdown, which results in faster charge dissipation. In environments with high humidity, adsorbed water molecules modify surface states and facilitate the creation of conductive water bridges, which enhance charge screening and decrease net output.<sup>77,78</sup> Rather than being a limitation, humidity can be strategically leveraged to enhance TENG performance. By combining hydrophobic dielectric selection with surface charge engineering, TENGs have maintained ~91% of their output at 90% RH, demonstrating the viability of humidity tuning as a stabilization way.<sup>79</sup> Controlled humidity levels are utilized to facilitate adaptive functionalities, including self-healing and mechanical stretchability. A notable example is a hydrogel-elastomer double-layer TENG, in which a carbon nanotube (CNT)-doped hydrogel electrode and a soft Ecoflex elastomer triboelectric layer allow conformal adhesion to skin, fast self-repair within 5 minutes, and stable operation under variable environmental conditions. The TENG shows an output voltage of 180 V, a peak current of 0.8  $\mu\text{A}$ , and a maximum power density of 37.8  $\text{mW m}^{-2}$ . These values are sufficient for the operation of small electronic devices, including LEDs and stopwatches, highlighting their applicability in wearable and self-sustaining sensing applications.<sup>80</sup> Furthermore, advanced hybrid architectures incorporating humidity-responsive

materials, like metal-organic frameworks (MOFs) or PVA/LiCl films, offer self-regulated and multi-stimuli energy harvesting capabilities.<sup>75</sup> One such composite maintains stable output even under harsh humidity and contamination conditions.

Building on these concepts, the recent hybridization of MEGs and TENGs has effectively handled their traditionally conflicting humidity requirements. Moisture-adaptive cellulose/MXene aerogels with interconnected porous architectures enable synergistic harvesting of moisture and triboelectric energy across a wide humidity range (20–90% RH). By combining the high current output of MEGs with the high voltage output of TENGs, this hybrid device delivers a maximum voltage of 106 V, an instantaneous current density of  $\sim 400 \mu\text{A cm}^{-2}$ , and an ultrahigh power density of  $\sim 77 \mu\text{W cm}^{-2}$ , surpassing most reported ambient energy harvesters.<sup>81</sup>

As a result, although conventional TENGs do not directly convert humidity into electricity, it is essential to understand and control the effects of environmental moisture for reliable implementation. This category also presents emerging opportunities for humidity-mechanical hybrid systems, especially for applications in wearable electronics and environmental monitoring.

Table 1 shows a full comparison of the four humidity-driven energy harvesting mechanisms discussed above. The table summarizes the key working principles, representative materials, output characteristics, and practical advantages and limitations of each class of devices. It further lists common application scenarios informed by the energy generation profile and the conditions of operation. This comparative overview aims to assist readers in recognizing the most appropriate mechanism for specific functional and environmental needs while emphasizing the design trade-offs present in each method.

### 3. Materials and architectures used

The performance of humidity-driven energy harvesting systems is intrinsically linked to the selection of materials and the architectural configuration of the device. The choice of material affects water absorption, ion transport, charge separation, and output stability, while the device design determines charge collecting efficiency and environmental adaptability. This section categorizes and examines the fundamental material classes and structural designs employed in the four primary processes of moisture-based energy harvesting, directing readers to Table 2 for illustrative experimental specifics.

#### 3.1 Carbon-based materials

Graphene oxide (GO), rGO, and CNTs are among the most frequently used materials in moisture-enabled generators due to their high surface area, tunable functional groups, and excellent ionic conductivity.<sup>82,83</sup> GO contains oxygen-rich functional groups, like -OH, -COOH, and epoxy groups, which dissociate in the presence of moisture to produce mobile ions. The layered architecture of GO facilitates directional ion



Table 2 Key materials and their configurations for humidity-driven energy harvesting systems

Material system	Architecture/configuration	Mechanism	Key performance metrics	Ref.
GO/rGO/CNT	Multilayer Ni/GO/GO-rGO/CNT/PET	Ion transport <i>via</i> functional groups and heterojunctions	$V_{OC}$ up to $\sim 735$ mV, $I_{SC} > 140$ $\mu$ A @ 80% RH	84
CNT-functionalized fiber mats	Electrospun PSF/PU + CNT bilayers	Capillary-driven ion migration	$V_{OC}$ : 419 mV, $I_{SC}$ : 1.5 mA, $P_{out}$ : 320 nW	85
<i>o</i> -CNT + vermiculite	Layered heterojunctions	Proton transport <i>via</i> nanochannels	$V_{OC}$ up to 735 mV (35–90% RH)	86
CNT-coated carbon cloth	Sandwich Zn plate/CNT-CC/filter paper	Evaporation-driven electron transport	Current density $> 1$ mA; $P_{dens}$ : 300 $\mu$ W $cm^{-2}$	88
Gelatin/MWCNT nanocomposite	Electrospun EF + PEDOT:PSS	Proton conduction <i>via</i> -COOH groups	$V_{OC}$ : 0.95 V, $I_{SC}$ : 51.7 $\mu$ A; wearable demo (face mask)	90
Hydrogels (PAMPS-PAAm, LiCl)	Crosslinked hydrogel thin films	Proton hopping + ionic diffusion	$V_{OC}$ : $\sim 0.87$ V; long-term stability $> 1400$ h	42
Engineered PAM-AMPS-LiCl hydrogel	Stretchable hydrogel	Proton conduction + ion mobility	$V_{OC}$ : 0.81 V, $J$ : 480 $\mu$ A $cm^{-2}$ ; 506% strain tolerance	96
P(AM-co-AA) hydrogel + MWCNT	Sandwich structure	Asymmetric EDL + ion migration	$V_{OC} \sim 1.2$ V, $I_{SC}$ : 10 $\mu$ A $cm^{-2}$	97
Metal oxides (ZnO, TiO <sub>2</sub> , SnO <sub>2</sub> )	Nanowires, thin films	Piezoelectric and conductivity modulation by humidity	$V_{OC}$ drops from 0.82 to 0.05 V (15–60% RH)	100
MoS <sub>2</sub> /GO composite	Screen-printed films on PET	Humidity-responsive conductivity	Response time 1.3 s; recovery 12 s (33–98% RH)	104
GO/polymer hybrids	GO/PVA nanofibers, GO/cellulose	Directional ion transport	98.44% response at 80% RH; stability 1 week; effective in respiration monitoring	105
MXene-hydrogel hybrids	Electrospun PVA/MXene nanofibers + MoSe <sub>2</sub> piezoelectric NG	Proton dissociation + conductivity	$\sim 40\%$ response; fast response/recovery (0.9/6.3 s); self-powered <i>via</i> MoSe <sub>2</sub> PENG (35 mV, 42 mW $m^{-2}$ )	106
Ionic hydrogel/AAO heterojunction	Hydrogel + AAO	Built-in E-field + proton migration	$V_{OC}$ 1.25 V, $I_{SC}$ 300 $\mu$ A $cm^2$ , $P_{dens}$ 71 mW $cm^{-2}$	70
PU@PSS/PEDOT:PSS/ITO	Nanoarchitected multilayer	Hygroscopic proton conduction	Current $> 100$ $\mu$ A; respiration sensing	107

transport and is easily integrated into flexible thin films and composite membranes.

As shown in Fig. 3a, a multilayer structure based on Ni/GO/GO-rGO/CNT/PET has been developed to enhance moisture-enabled energy harvesting performance.

Increasing the proportion of rGO in the composite leads to improved output voltage and current caused by optimized conductivity and ion mobility, with optimal performance noted at a GO : rGO ratio of 10 : 1. Fig. 3b and c illustrates that GO/rGO heterojunctions yield a more stable voltage output and markedly increased short-circuit currents ( $>140$   $\mu$ A at 80% RH) in comparison to pure GO, highlighting the importance of heterojunction engineering for robust long-term performance.<sup>84</sup> The addition of CNTs into polymeric substrates greatly improves ionic conductivity by promoting aligned water-mediated proton pathways and enhancing surface wettability. A notable example is a CNT-functionalized electrospun polysulfone/polyurethane (PSF/PU) mat, modified *via* oxygen plasma and coated with alternating polyelectrolytes and CNT bilayers. As illustrated in Fig. 3d–f, this stretchable moisture-driven power generator (MPG) generated spontaneous directional ion migration along the CNT-coated fibers, achieving a power output of 320 nW. These dynamic profiles demonstrate

the significance of CNT heterostructures in sustaining high output despite mechanical deformation.<sup>85</sup>

Strong heterojunctions that integrate oxidized CNTs (*o*-CNTs) with vermiculite (VM) membranes exhibit stable performance characteristics. In this system (Fig. 3g–i), VM nanochannels provide proton-selective transport, while moisture-driven cycles between *o*-CNT/VM layers allow for voltage production, even in overlapping topologies. Output voltage increased from 492 to 735 mV as RH increased from 35 to 90%, underscoring the humidity responsiveness of such heterojunctions.<sup>86</sup>

Carbon cloth (CC) and activated carbon fibers have wide applications in MEGs and evaporation-induced energy systems. Their primary functions include acting as current collectors and providing porous scaffolds that improve moisture absorption, ionic transport, and charge transfer efficiency. Their highly porous structure and intrinsic conductivity make them ideal for enhancing electrochemical interactions at the solid-vapor interface, especially in humidity-powered devices.<sup>87–89</sup> In addition to their structural functionality, carbon-based materials are preferred for their mechanical flexibility, chemical stability, and compatibility with printing or coating processes.





**Fig. 3** Humidity-enabled energy harvesting based on carbon-based materials. (a) Schematic of a multilayer heterojunction device composed of Ni/GO/GO-rGO/CNT/PET, showing the engineered layer-by-layer structure designed to optimize charge transport and moisture interaction. © 2024 Wiley-VCH. Reproduced with permission from ref. 84. (b) Output voltage behavior of the pristine GO and GO/rGO hybrid devices under high relative humidity, demonstrating improved stability and enhanced performance with the addition of rGO. © 2024 Wiley-VCH. Reproduced with permission from ref. 84. (c) Short-circuit current as a function of relative humidity (RH), reaching over 140  $\mu\text{A}$  at 80% RH, confirming the moisture-sensitivity and strong enhancement of electric output in the GO/rGO-based devices. © 2024 Wiley-VCH. Reproduced with permission from ref. 84. Layered GO/rGO heterojunctions significantly improve output stability and current generation by enhancing moisture-assisted ion transport and interfacial charge collection. (d) Schematic of the CNT-based MPG operation showing water-driven capillary flow and ion migration. © 2023 RSC. Reproduced with permission from ref. 85. (e) Electrospun PSF/PU fiber mats are plasma-treated, modified with bPEI, and spray-coated layer-by-layer with PDDA/PSS and charged MWCNTs. © 2023 RSC. Reproduced with permission from ref. 85. (f) Time-dependent  $V_{\text{OC}}$ ,  $I_{\text{SC}}$ , and power output of the MPG with 15 MWCNT bilayers. © 2023 RSC. Reproduced with permission from ref. 85. Hierarchically structured CNT-based fiber generators leverage capillary-driven water transport to achieve stable, continuous power generation under humid conditions. (g) Schematic of the o-CNT/vermiculite (VM) heterojunction device connected by copper wires and conductive silver paste. © 2024 Elsevier. Reproduced with permission from ref. 86. (h) Moisture absorption by VM leads to  $-\text{OH}$  dissociation and proton release, while evaporation at the o-CNT surface drives directional ion flow through VM nanochannels. © 2024 Elsevier. Reproduced with permission from ref. 86. (i) Output voltage increases from 492 mV to 735 mV as RH rises from 35 to 90%, confirming the moisture-responsive behavior of the device. © 2024 Elsevier. Reproduced with permission from ref. 86. Nanochannel-enabled ion transport in CNT-clay heterojunctions enables high humidity sensitivity and scalable voltage output.

Carbon compounds are typically integrated with ionic polymers, gelatin, or conducting polymers to improve their performance in humid conditions. These combinations enhance ion mobility, hydrophilicity, and device stability in fluctuating environments. In some studies, CNT-functionalized CC was used in a hydroelectric generator, which significantly enhanced evaporation-driven electron transport. The nanostructured CNT coating promoted charge separation and considerably increased the evaporation surface area, consequently boosting water transport and power output.

As shown in Fig. 4a, a CNT-coated CC hydroelectric generator functioned as a sandwich of Zn plate/CNT-CC/filter paper. The diaphragm functions to absorb and store water, thereby providing a consistent moisture supply to the CC surface, which is critical for ongoing evaporation-driven operation. To optimize performance, different CNT deposition configurations were evaluated. Optimized CNT deposition significantly increased current density ( $>1$  mA, Fig. 4b) though high ambient humidity suppressed evaporation and reduced output (Fig. 4c). These results indicate that high levels of ambient humidity hinder water evaporation,





Fig. 4 Moisture-enabled energy harvesting based on evaporation-driven and proton-conducting architectures. (a) Schematic of a moisture-enabled device with a sandwich structure composed of a zinc plate, CNT-coated carbon cloth (CC), and a hydrophilic filter paper diaphragm for sustained water evaporation and charge separation. © 2024 The American Chemical Society. Reproduced with permission from ref. 88. (b) Comparative water evaporation and charge separation of devices using original CC, bottom-CNT-coated CC, and top-CNT-coated CC, showing superior performance when CNTs are added to the upper surface. © 2024 The American Chemical Society. Reproduced with permission from ref. 88. (c) Effect of ambient humidity on current output at 20%, 50%, and 95% RH, indicating reduced performance at high humidity due to suppressed evaporation. © 2024 The American Chemical Society. Reproduced with permission from ref. 88. These results highlight that evaporation-driven architectures rely critically on interface positioning and ambient humidity to maximize moisture-induced charge separation and current output. (d) Schematic of the MEG showing ion generation and migration via proton hopping and charge redistribution across the MG-EF/PEDOT:PSS structure. © 2022 Elsevier. Reproduced with permission from ref. 90. (e) Current–voltage characteristics of MEGs based on EF, M-EF, G-EF, and MG-EF under 90% RH. © 2022 Elsevier. Reproduced with permission from ref. 90. (f) Electrical conductivity of the MG-EF nanocomposite increases with relative humidity (10–90%). © 2022 Elsevier. Reproduced with permission from ref. 90. (g) A wearable KF94 face mask integrated with an MEG module that harvests power from human breath moisture. © 2022 Elsevier. Reproduced with permission from ref. 90. This study demonstrates the feasibility of integrating humidity-driven generators into wearable platforms, leveraging breath moisture for continuous, self-powered operation.

consequently limiting the device's power-generating capacity. The optimized configuration attained a power density of  $300 \mu\text{W cm}^{-2}$  and generated currents reaching 4 mA, making it appropriate for powering small electronic devices.<sup>88</sup>

Another hierarchical nanocomposite combined gelatin-coated electrospun fibers with multi-walled carbon nanotubes (MWCNTs) and a poly(3,4-ethylenedioxythiophene):polystyrene sulfonate (PEDOT:PSS) layer. In this case, oxygen-rich groups generated protons during hydration, while PEDOT:PSS improved charge separation (Fig. 4d). The device exhibited an exceptional  $I$ – $V$  response (Fig. 4e) and a humidity-dependent conductivity that escalated from  $8.42 \text{ nS cm}^{-1}$  at 10% RH to  $2.55 \text{ mS cm}^{-1}$  at 90% RH (Fig. 4f). Integrated into a KF94 face mask, the module

successfully harvested respiration moisture to power LEDs (Fig. 4g), maintaining performance over >10 000 bending cycles.<sup>90</sup>

These results highlight that designed carbon composites, via heterojunctions, CNT integration, or polymer hybrids, attain steady and flexible power production, which is particularly ideal for wearable, printable, and adaptive devices (Table 2).

### 3.2 Polymeric and hydrogel systems

Polymers offer remarkable adaptability in humidity-responsive energy systems thanks to their tunable chemistry, mechanical flexibility, and capacity to hold significant amounts of water. Commonly used polymers include polyvinyl alcohol (PVA), polyaniline (PANI), polypyrrole (PPy), and polyacrylamide





**Fig. 5** Moisture-based electric generation from sulfonated hydrogel systems. (a) Schematic of the UV-assisted synthesis of SHMEG using the PAMPS-g-PAAm hydrogel with AMPS, AAm, PEGDA, and LiCl to enhance proton dissociation and water transport. © 2025, Wiley-VCH. Reproduced with permission from ref. 42. (b) Short-circuit current response of SHMEG under different RH levels (10–90%), showing two orders of magnitude enhancement. © 2025, Wiley-VCH. Reproduced with permission from ref. 42. (c) Long-term output performance of SHMEG under ambient conditions, maintaining  $\sim 0.867$  V for over 1400 h. © 2025, Wiley-VCH. Reproduced with permission from ref. 42. (d) Demonstration of a wearable application using printed SHMEG circuits on textiles, enabling power delivery to on-body wireless electronics. © 2025, Wiley-VCH. Reproduced with permission from ref. 42. This study demonstrates that sulfonated hydrogels can achieve long-term, stable humidity-driven power generation while remaining compatible with wearable and textile-based electronics. (e) Schematic of a molecular-engineered hydrogel (MEH) integrating PAM, AMPS, and LiCl for enhanced ion generation and transport via sulfonic acid groups and lithium ions. © 2023, Wiley-VCH. Reproduced with permission from ref. 96. (f) Output characteristics of MEH-MEG under various humidity levels, showing optimal performance across 30–90% RH with a decline at 100% RH due to gradient loss. © 2023, Wiley-VCH. Reproduced with permission from ref. 96. (g) Demonstration of MEH-MEG integrated into a face mask for real-time respiration monitoring. © 2023, Wiley-VCH. Reproduced with permission from ref. 96. (h) Practical application of MEH-MEGs in smart wearable systems, such as protective helmets and medical suits, powered by humidity from human breath. © 2023, Wiley-VCH. Reproduced with permission from ref. 96. These results highlight the importance of molecular-level hydrogel design in balancing ion mobility and humidity gradients for reliable wearable energy harvesting. (i) Schematic of a sandwich-structured MEG integrating  $\text{Li}^+$ -doped MWCNT electrodes and P(AM-co-AA) hydrogel, leveraging asymmetric EDLs and humidity gradients. © 2025, Elsevier. Reproduced with permission from ref. 97 (j) Output performance under varying RH, showing peak voltage (1.2 V) and current ( $10 \mu\text{A cm}^{-2}$ ) at 85% RH, with performance decline beyond 95% RH. © 2025, Elsevier. Reproduced with permission from ref. 97. (k) Demonstration of 12 MEG units in a series powering a calculator and an LED. © 2025, Elsevier. Reproduced with permission from ref. 97. This work demonstrates scalable voltage amplification and practical load powering through the modular integration of hydrogel-based MEGs.





**Fig. 6** Metal oxides and semiconductors for humidity-responsive energy harvesting. (a) Schematic of a self-powered humidity sensor based on Al-doped ZnO nanowires (Al-ZnO NWs) grown on a Ti foil, featuring a sandwich structure with an Al counter electrode and Kapton supports. © 2014, The Royal Society of Chemistry. Reproduced with permission from ref. 100. (b) Piezoelectric output voltage under different relative humidity levels (15–60% RH), highlighting the humidity-sensitive nature of Al-ZnO NWs. © 2014, The Royal Society of Chemistry. Reproduced with permission from ref. 100. (c) Moisture adsorption and the Grotthuss-type proton hopping mechanism that leads to the screening of polarization charges, thereby reducing output voltage. © 2014, The Royal Society of Chemistry. Reproduced with permission from ref. 100. This study reveals that humidity-induced proton transport can modulate piezoelectric polarization in ZnO nanostructures, enabling self-powered humidity sensing and imposing intrinsic output limitations at high moisture levels. (d) Schematic of the MoS<sub>2</sub>/GO composite structure, highlighting water molecule diffusion dynamics. © 2024, The Royal Society of Chemistry. Reproduced with permission from ref. 104. (e) Fabrication of a flexible PET-based humidity sensor using screen-printed interdigital electrodes and layer-by-layer drop coating of MoS<sub>2</sub>/GO dispersion. © 2024, The Royal Society of Chemistry. Reproduced with permission from ref. 104. (f) Stepwise humidity sensing response showing high reversibility and rapid absorption–desorption between 33% and 98% RH. © 2024, The Royal Society of Chemistry. Reproduced with permission from ref. 104. This work demonstrates that 2D semiconductor–oxide composites can deliver fast, reversible, and mechanically flexible humidity-responsive electrical signals suitable for wearable and distributed sensing platforms.

(PAAm), as well as biopolymers like cellulose and chitosan. Hydrogels, including crosslinked polymer networks capable of absorbing and retaining substantial quantities of water, are particularly efficient in energy production powered by humidity.<sup>91–94</sup> The porous framework of the hydrogel enables effective capillary-driven water transport, while embedded sulfonic acid groups and LiCl improve ion dissociation and mobility in humid environments. Fig. 5a–d shows a poly(2-acrylamido-2-methyl-propane-sulfonic acid-co-acrylamide) (PAMPS-PAAm) hydrogel SHMEG device that demonstrated *I*<sub>SC</sub> increasing from 0.05 to 69.4 μA as RH increased from 10 to 90%, sustained ~0.867 V output for over 1400 h in fluctuating RH,

and enabled scalable integration into textiles for moisture harvesting from sweat to power chargers.<sup>42</sup>

Very recently, rechargeable moisture-enabled electricity cells employing dual functional layers and redox-assisted self-repair mechanisms have demonstrated stable power generation for over 2080 h, with an output voltage near 1.08 V and a peak power density of ~5.83 μW cm<sup>-2</sup>. This record performance suggests that active regeneration strategies may be key to overcoming intrinsic lifetime limitations in moisture-driven energy harvesters and moving toward practical long-life applications.<sup>95</sup>



Molecular engineering strategies have enabled the design of highly stretchable and flexible MEGs by integrating sulfonic acid-functionalized hydrogels with lithium ions. Fig. 5e and f illustrates that molecular-engineered hydrogel (MEH) devices made from polyacrylamide (PAM), 2-acrylamido-2-methylpropane sulfonic acid (AMPS), and LiCl produced 0.81 V and  $480 \mu\text{A cm}^{-2}$ . These devices maintained functionality under 506% strain and demonstrated efficient operation across an RH range of 30–100%, with only a slight performance decline at full humidity. Their adaptability facilitated integration into wearable systems, where integration into masks and protective equipment permitted respiration-driven energy harvesting (Fig. 5g and h).<sup>96</sup> Similarly, the optimization of the hydrogel-electrode interface using Li<sup>+</sup>-doped MWCNT/P(AM-co-AA) (acrylamide-co-acrylic acid copolymer) sandwich structures

improved asymmetric EDL effects and humidity-driven ion transport, resulting in 1.2 V and  $10 \mu\text{A cm}^{-2}$  at 85% RH, with consistent performance spanning 45–85% RH (Fig. 5i and j). Although outputs declined at >95% RH, 12 devices in series powered LEDs and calculators (Fig. 5k).<sup>97</sup> Other ionic hydrogels, such as PVA-phytic acid-glycerol, maintained continuous operation ( $\sim 1000$  h) and enabled scalable assemblies reaching 210 V.<sup>98</sup>

Recent hydrogel-based MEG designs have demonstrated substantially enhanced output performance, addressing the long-standing limitation of low power density in polymeric systems. A high-power hydrogel-based moisture-electric generator incorporating rGO nanosheet channels and LiCl hygroscopic components achieved an open-circuit voltage of approximately 0.6 V and a short-circuit current density of  $\sim 0.58$

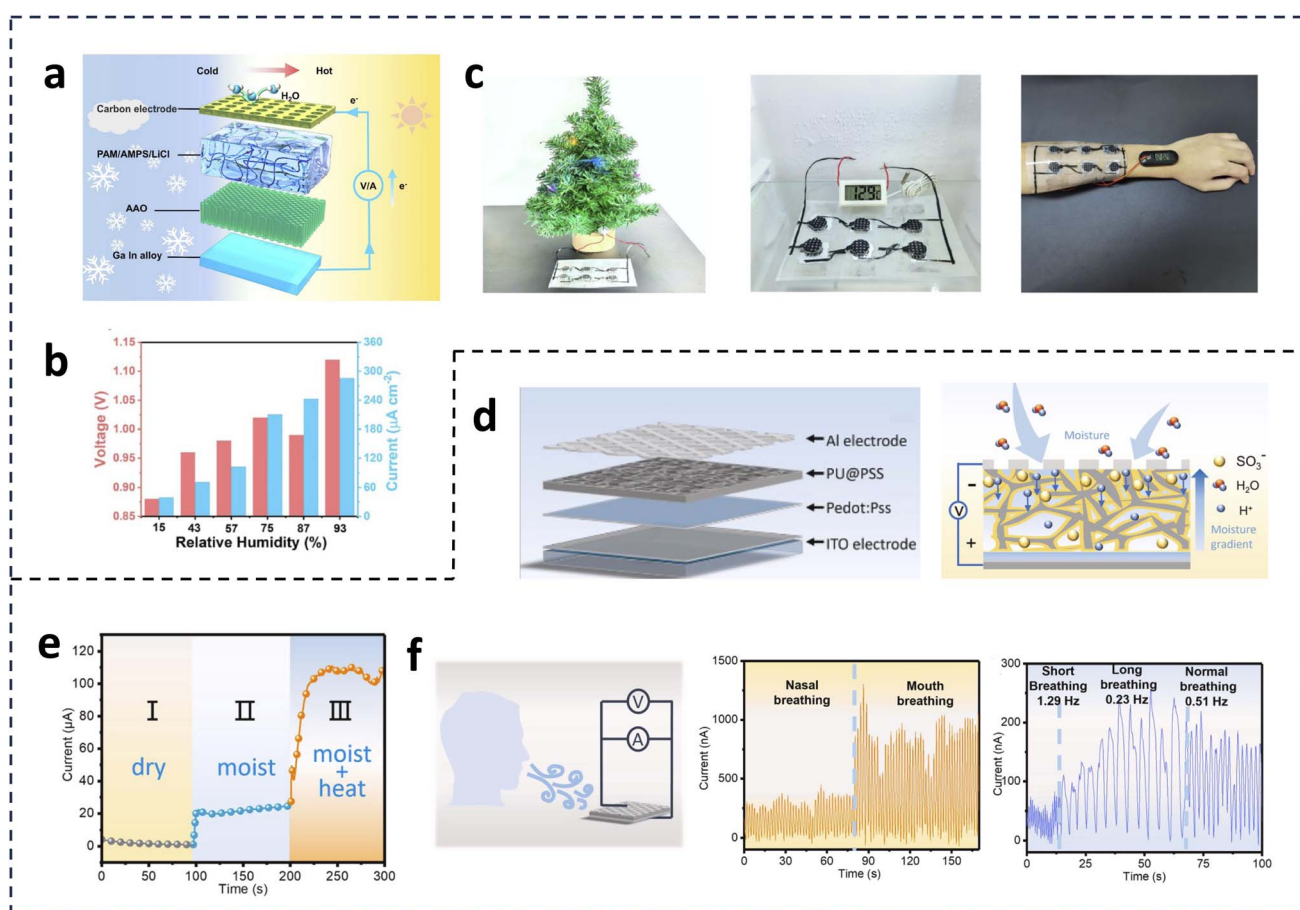


Fig. 7 Composite and hybrid structures for humidity-responsive energy harvesting. (a) Schematic of the ionic hydrogel/AAO-based moisture-enabled power generator composed of a PAM/AMPS/LiCl hydrogel, AAO film, carbon black top electrode, and gallium–indium alloy bottom electrode. © 2023, The Royal Society of Chemistry. Reproduced with permission from ref. 70. (b) Electrical output performance under different humidity levels, achieving 1.25 V and  $300 \mu\text{A cm}^{-2}$  at 93% RH. © 2023, The Royal Society of Chemistry. Reproduced with permission from ref. 70. (c) Demonstration of real-world applications, including powering a decorative light, refrigerator thermometer, and electronic watch. © 2023, The Royal Society of Chemistry. Reproduced with permission from ref. 70. This work demonstrates that combining ionic hydrogels with ordered nanoporous AAO supports can yield high-output, scalable humidity-driven generators capable of directly powering small electronic devices. (d) Schematic of the MEG design using a porous PU@PSS composite layer, PEDOT:PSS ion interception layer, and gridded Al/Ito electrodes enabling directional ion diffusion and DC generation. © 2024, Elsevier. Reproduced with permission from ref. 107. (e) Temperature-enhanced output under thermal radiation (>100  $\mu\text{A}$ ) due to increased ion mobility. © 2024, Elsevier. Reproduced with permission from ref. 107. (f) Self-powered respiration monitoring with distinguishable electrical signals from mouth vs. nasal breathing, highlighting application in wearable health sensors. © 2024, Elsevier. Reproduced with permission from ref. 107. This study highlights how multilayer ion-interception designs and thermal coupling can enable multifunctional MEGs that simultaneously harvest environmental moisture and physiological signals.



mA cm<sup>-2</sup> at 80% RH. Notably, this output level surpasses that of many previous hydrogel MEGs, which regularly rely on large-area devices or extensive series/parallel configurations to reach comparable current levels. These results demonstrate that rational ion-transport network design and water-retention engineering can substantially elevate the power density of hydrogel MEGs, expanding their applicability to flexible and high-performance energy harvesting systems.<sup>99</sup>

Polymeric and hydrogel systems together offer scalable, stretchable, and wearable platforms, revealing resilience and adaptability in various settings (Table 2). This section focuses on polymeric and hydrogel systems from functional and performance-oriented perspectives. Bioinspired and biomass-derived polymers are discussed separately in Subsection 3.6 to highlight sustainability considerations.

### 3.3 Metal oxides and semiconductors

Semiconducting and dielectric metal oxides, such as ZnO, TiO<sub>2</sub>, SnO<sub>2</sub>, and MoS<sub>2</sub>, exhibit promise in hygroelectric systems thanks to their sensitivity to the surface adsorption of water molecules. These materials change their surface potential and electrical conductivity based on humidity, allowing for the direct modulation of electrical signals by ambient moisture.

Fig. 6a–c demonstrates that Al-doped ZnO nanowire generators possess significant humidity sensitivity, as evidenced by a reduction in output voltage from about 0.82 V at 15% RH to around 0.05 V at 60% RH, owing to water adsorption and ion-mediated screening of polarization charges.<sup>100</sup> Cd- and Co-doped ZnO nanowires confirmed similar humidity-induced suppression of piezoelectric performance.<sup>101,102</sup> These systems demonstrate the way the structural and dopant engineering of ZnO influences its surface states when exposed to moisture. TiO<sub>2</sub> and SnO<sub>2</sub> films exhibit reversible conductivity alterations following water adsorption, as supported by self-consistent charge density-functional tight-binding (SCC-DFTB) simulations.<sup>103</sup> These effects are exploited in moisture-sensitive power generators or self-powered sensors using thin TiO<sub>2</sub> or SnO<sub>2</sub> films, where moisture alters electronic conductivity at the surface layer. Layered MoS<sub>2</sub>/GO composites further combine high surface area and hydrophilicity, enabling rapid response (1.3 s), recovery (12 s), and stability across 33–98% RH on flexible PET substrates (Fig. 6d–f).<sup>104</sup>

Overall, semiconductors and oxides function not only as humidity-sensitive active layers but also as interfacial electrolytes or charge-modulating coatings in hybrid MEGs (Table 2).

### 3.4 Composite and hybrid structures

To overcome the limitations of single-component systems, composite and hybrid materials have gained increasing attention in humidity-enabled energy harvesting. These materials integrate the advantages of various components to improve charge generation, ion mobility, and structural durability. One such approach involves combining GO with polymers, like PVA or cellulose, which significantly improves both mechanical integrity and humidity responsiveness. GO/PVA nanofiber composites developed through electrospinning show notable

sensitivity at 80% relative humidity, providing stable performance over long durations thanks to improved water absorption and directional ion transport facilitated by the layered structure of GO.<sup>105</sup>

The integration of metal oxides, such as Ti<sub>3</sub>C<sub>2</sub>T<sub>x</sub> MXenes, into polymeric hydrogels has resulted in the creation of multifunctional hybrids that function through both piezoelectric and hygroelectric mechanisms. These systems leverage the hydrophilic properties of hydrogels and the superior electrical conductivity of the included nanosheets, facilitating rapid and reproducible power generation under humid conditions.<sup>106</sup> More complex designs include hydrogel/AAO heterojunctions (Fig. 7a–c), where built-in fields enhance proton migration to deliver 1.25 V and 71 mW cm<sup>-2</sup> peak power.<sup>70</sup> Likewise, nano-architected PU@PSS/PEDOT:PSS/ITO multilayers (Fig. 7d–f) combined porous PU and sulfonic acid groups to boost ion mobility, yielding >100 μA under humid or thermally stimulated conditions and functioning as a self-powered respiration sensor with signal ranges from tens of nA to nearly 1 μA.<sup>107</sup>

Recent advances have investigated bioinspired and ion-enhanced composites, including salt-hydrogel hybrids and leaf-like moisture channel designs. These systems use hygroscopic salts or ionic liquids to improve moisture adsorption and ion conductivity while mimicking natural fluid pathways to facilitate directional charge movement and maintain stable power output. These solutions have shown efficacy in enhancing energy density and reliability across diverse environmental factors.<sup>70</sup>

Beyond material-level design, system-level architectural innovation has enabled multistage and modular moisture-enabled generators with customizable electrical outputs. A representative multistage water-enabled electric generator integrates liquid flow and moisture diffusion layers within a single device, achieving a maximum power density of ~92 mW m<sup>-2</sup> (~11 W m<sup>-3</sup>). Through series and parallel integration, output voltages greater than 10 V and currents exceeding roughly 280 μA have been demonstrated under real outdoor conditions, highlighting the scalability and versatility of multistage water-based energy harvesting systems.<sup>108</sup>

Overall, composite and hybrid structures enable precise control over moisture diffusion, charge separation, and interfacial transport using approaches such as layer-by-layer assembly, core-shell morphology, and functional gradient design. These innovations play a vital role in enhancing high-performance, durable, and miniaturized humidity-responsive energy harvesting systems that are suitable for practical applications.

A summary and comparison of the representative materials and device architectures for humidity-driven energy harvesting systems are listed in Table 2.

### 3.5 Conflicting results and challenges in scaling

Although rapid progress has been achieved, the literature also contains contradictory findings and reports of failures to scale. For example, graphene oxide-based films have been reported with open-circuit voltages as low as tens of millivolts<sup>84</sup> and as



high as several volts,<sup>85,86</sup> even under nominally similar humidity conditions. This spread suggests a strong dependence on uncontrolled factors such as residual oxygen functional groups, electrode configuration, and ambient cycling.

A major source of inconsistency in reported humidity-driven electrical outputs arises from electrode-induced artifacts. Recent studies have shown that the use of dissimilar electrodes can introduce voltage contributions originating from differences in standard electrode potentials, galvanic effects, or contact potential differences, which may be mistakenly attributed to humidity-driven mechanisms. Zheng *et al.* systematically showed that electrode material selection alone can dominate the observed output in so-called hydrovoltaic systems, even in the absence of active moisture-induced ion transport.<sup>109</sup> Similarly, Yan *et al.* discovered that non-noble-metal electrodes can generate spurious voltage signals under humid conditions due to electrochemical reactions rather than intrinsic moisture–material interactions.<sup>110</sup> These findings highlight the necessity of rigorous control experiments, including the use of symmetric electrodes, inert electrode materials, and humidity-independent baseline measurements, to ensure that the measured output genuinely originates from humidity-driven processes rather than electrode chemistry.

Hydrogels illustrate another inconsistency: although sulfonated PAMPS-based systems have demonstrated continuous operation for over 1400 h,<sup>42</sup> many ionic gels and hydrogel composites dry out within 12–24 h under low humidity.<sup>96,98</sup> Similarly, textile-based carbon cloth devices and stacked hydrogel modules show promising integration,<sup>88,89</sup> but their areal power densities typically fall one to two orders of magnitude below lab-scale prototypes. Hybrid and composite designs provide synergistic perspectives: GO-hydrogel heterostructures augment proton conduction and output,<sup>44</sup> while CNT-polymer scaffolds promote flexibility and charge transport.<sup>85</sup> Nevertheless, despite these promising advancements, many physically intricate systems demonstrate heightened resistance or inconsistent drying, which diminishes overall efficiency.<sup>104</sup> Across all material classes, comparisons are further complicated by the lack of standardized test protocols—device area, RH, airflow, and temperature are reported inconsistently, hindering reproducibility. These conflicting outcomes highlight the urgent need for benchmarking protocols, long-term durability testing, and transparent reporting of both successes and failures to guide the practical scaling of moisture- and evaporation-driven electricity generation.

### 3.6 Bioinspired and sustainable materials

In addition to synthetic polymers and inorganic nanomaterials, bioinspired and biomass-derived materials are becoming an essential type of functional components for humidity-driven energy harvesting systems. These materials are focused on being sustainable, biodegradable, and compatible with the environment. Natural polymers, including chitosan, cellulose, alginate, silk fibroin, and lignocellulosic composites, contain numerous hydrophilic functional groups (*e.g.*,  $-\text{OH}$ ,  $-\text{NH}_2$ , and  $-\text{COOH}$ ) that enhance water adsorption and proton transport,

rendering them inherently appropriate for humidity-driven ion migration mechanisms.<sup>93</sup>

Chitosan-based hydrogels exhibit stable moisture-induced voltage generation *via* proton conduction along hydrogen-bonded networks while providing benefits such as biocompatibility, low toxicity, and renewability.<sup>111</sup> Similarly, films derived from cellulose and nanofibrillated cellulose composites exhibit remarkable humidity absorption and directed ion transport, attributed to their hierarchical porosity and surface chemistry.<sup>112</sup> Lignocellulosic materials provide mechanical strength and scalability processing capabilities, allowing large-area or flexible device architectures.<sup>113,114</sup>

From an environmental perspective, these bioinspired systems offer clear benefits compared to traditional synthetic materials, including reduced life-cycle environmental impact, biodegradability, and compatibility with sustainable production processes.<sup>115,116</sup> However, performance trade-offs are still obvious. Biomass-derived materials generally exhibit lower electrical conductivity, reduced long-term stability under extreme humidity cycling, and narrower operating voltage ranges compared to optimized synthetic polymers or inorganic nanostructures.<sup>117</sup> Strategies such as bio-inorganic hybridization, crosslinking, surface functionalization, and incorporation of benign ionic additives have therefore been explored to bridge the performance gap while retaining sustainability advantages.<sup>93</sup>

In general, bioinspired and biodegradable materials represent a promising pathway for the development of environmentally sustainable humidity-driven energy harvesters. This is particularly applicable to transient electronics, wearable systems, and distributed sensing platforms, where sustainability and end-of-life issues are very important.

### 3.7 Device architectures and electrode design

Humidity-driven devices utilize several structural configurations to optimize moisture interaction and charge transport. Sandwich-type architectures commonly position a hygroscopic active layer between two electrodes, a format that supports directional ion transport and efficient charge collection. The high-output device mentioned in Fig. 7d–f utilizing a PU@PSS composite with a gridded aluminum electrode and PEDOT:PSS interlayer serves as a notable example of the effectiveness of this configuration.<sup>107</sup> Planar devices, such as inkjet-printed humidity sensors with interdigitated silver electrodes, utilize hydrophilic substrates and printed electrode designs to enable cost-effective, large-area production and rapid response times. These systems exhibit effective self-powered operation and maintain performance despite repeated mechanical deformation, which is well-suited to flexible and wearable applications. Recent work developed a fully printed, flexible, and self-powered humidity sensor based on paper substrates and screen-printed electrodes, demonstrating the feasibility of low-cost, customizable 2D layouts with excellent mechanical flexibility and high voltage output (up to 1.03 V) across a wide humidity range (11–95% RH).<sup>118</sup> Another work used a nanofibrillated cellulose/GO aerogel over patterned electrodes. It



showed ultra-high capacitance sensitivity ( $\sim 6576$  pF/% RH), a rapid response time of 57 s, a recovery time of 2 s, and great flexibility and reproducibility.<sup>119</sup> Fiber-based or textile-integrated formats, including MWCNT/PEDOT:PSS-coated cotton fabrics, improve mechanical flexibility and enable stable energy output under deformation.<sup>120</sup>

Electrode materials and geometries are crucial to device performance. Common materials include gold, silver, ITO, carbon paper, and conductive textiles. Interdigitated and asymmetric electrode configurations, commonly produced *via* inkjet, screen, or roll-to-roll printing, enhance active surface area, diminish internal resistance, and influence electric field distribution.<sup>121</sup> A design employing carbon ink on filter paper operated as a self-powered humidity-sensitive electrode, producing 0.19 V while staying flexible after more than 1000 bends.<sup>122</sup> In an alternative design, screen-printed BC/AC/MgCl<sub>2</sub> electrodes on polyimide (PI) substrates were fabricated using syringe-assisted direct writing, enabling fine control of electrode spacing and moisture diffusion pathways.<sup>123</sup>

These device structures are compatible with scalable manufacturing techniques, including solution casting, electrospinning, vacuum filtration, and inkjet or screen printing, which enable cost-effective and flexible production methods.<sup>121</sup> Such scalable fabrication methods, when integrated with optimized architectures and electrode designs, establish a viable basis for real-world humidity energy harvesting technologies.

**3.7.1 Scalable manufacturing and large-area fabrication strategies.** The effective implementation of humidity-driven energy harvesters, based on the device architectures and electrode designs outlined in Subsection 3.7, is fundamentally contingent upon their alignment with scalable, economical, and environmentally sustainable manufacturing techniques. Recent studies have demonstrated that many humidity-responsive materials and device architectures are inherently compatible with solution-based and printing-enabled fabrication methods, offering a realistic pathway from laboratory-scale demonstrations to large-area and high-throughput production.<sup>124</sup>

Scalable manufacturing approaches, such as roll-to-roll processing, spray coating, inkjet printing, screen printing, and electrospinning, have been widely adopted in the fabrication of moisture- and ion-driven energy devices. Inkjet- and screen-printed electrode patterns on paper, polymer, and textile substrates enable rapid, low-cost fabrication of planar and interdigitated architectures while preserving mechanical flexibility and reproducibility.<sup>121</sup> Paper- and textile-based platforms further provide intrinsic porosity and moisture permeability, which are advantageous for maintaining humidity gradients across extended areas. Roll-to-roll-compatible coating and printing techniques enable continuous production over meter-scale substrates, a key requirement for commercialization.

Several humidity-driven energy harvesting systems have successfully demonstrated scaling from millimeter-scale laboratory prototypes to centimeter-scale devices using printing- and coating-based approaches. Graphene oxide-based, hydrogel-based, and MOF-derived humidity harvesters fabricated *via* spray coating, vacuum filtration, and printing have

achieved active areas ranging from several cm<sup>2</sup> to tens of cm<sup>2</sup> while maintaining stable voltage output under ambient conditions. These experiments confirm the viability of advancing humidity-driven energy harvesting from proof-of-concept devices to practically applicable form factors; however, enlarging the area presents issues concerning humidity gradient uniformity and electrical interconnection.

Electrospinning, vacuum filtering, and continuous coating can produce porous nanofiber membranes and aerogel-like films with a high surface area, variable thickness, and interconnected pore networks. Water adsorption, ion transport, and electrical output depend on such microstructures. Notably, electrospinning has already achieved industrial-scale implementation for filtration, energy storage, and sensing applications, thereby highlighting its potential for humidity-driven energy harvesting devices.<sup>125,126</sup>

Ink formulation and rheological control represent additional bottlenecks in large-area manufacturing. Humidity-responsive materials must be processed into stable inks with controlled viscosity, surface tension, and drying kinetics to avoid coffee-ring effects, pore collapse, or phase segregation during printing. Water-based and low-toxicity solvent systems are particularly attractive for scalable and sustainable processing although they impose stricter constraints on film uniformity and mechanical robustness.<sup>121</sup>

Process-induced microstructural variations present further challenges during scale-up. Large-area fabrication can alter pore size distribution, interfacial adhesion, and electrode continuity relative to laboratory-scale casting, directly affecting moisture adsorption gradients and ionic transport pathways. Consequently, scalable humidity-driven devices must tolerate thickness nonuniformities and environmental fluctuations without catastrophic loss of performance.<sup>127,128</sup>

At the system level, large-area deployment introduces challenges related to electrical interconnection, impedance matching, and encapsulation.<sup>110,128,129</sup> Efficient series-parallel integration is required to translate material-level power density into usable voltage and current outputs.<sup>130</sup> Encapsulation strategies must balance environmental protection with controlled water vapor permeability, as excessive sealing suppresses device operation while insufficient protection accelerates degradation.<sup>131</sup> This trade-off is unique to humidity-driven energy harvesting and remains a key challenge for long-term operation.

Finally, scalability must be evaluated from techno-economic and sustainability perspectives. Several high-performance laboratory demonstrations depend on hydrated hydrogels, noble metals, or precisely regulated humidity conditions, which are unsuitable for large-scale production due to financial and practical limitations. Future scalable systems must emphasize the use of earth-abundant materials, low-temperature processing, reduced chemical complexity, and alignment with circular manufacturing principles to meet feasible costs, durability, and environmental targets.



## 4. Integration with energy storage

Although humidity-driven energy harvesting devices show promise in turning ambient moisture into electrical energy, the intermittent and low-density characteristics of the harvested energy restrict their practical application. Most humidity-based harvesters generate power in response to changing environmental conditions, including variations in humidity, temperature, and airflow. As a result, without a stable means of energy storage, these systems cannot reliably power electronic devices with continuous or burst energy demands. Integrating energy storage components into humidity-driven systems is therefore essential for realizing self-sustained and autonomous power platforms.

Hybrid harvesting platforms that integrate moisture-driven hydrovoltaic generators with photovoltaics are an efficient approach to improving total energy availability and system stability. A recent study demonstrated a cellulose-based moisture-driven hydrovoltaic device (MHD) integrated with a photovoltaic (PV) panel through an interfacial hydrogel layer that simultaneously enables evaporative cooling and hydrovoltaic energy generation. This configuration delivered a stable voltage of approximately 0.7 V and a power density of  $\sim 20 \text{ mW m}^{-2}$  over continuous operation for 30 days while increasing the hydrovoltaic output by  $\sim 150\%$  and improving PV efficiency by up to  $\sim 15\%$  through thermal regulation and waste-heat utilization. Such hybrid moisture-solar systems can directly support energy storage modules and autonomous operation of low-power electronics, illustrating the potential of multi-source integration in self-powered platforms.<sup>132</sup>

This section explores the latest methodologies for integrating energy storage, particularly supercapacitors and microbatteries, into humidity-responsive harvesters. Focus is directed towards the compatibility of materials, the integration of structures, and the synergistic performance between the energy generation and storage modules.

### 4.1 Supercapacitor integration

Supercapacitors, or electrochemical capacitors, are ideally compatible with humidity harvesters due to their higher power density, rapid charge and discharge capabilities, and extended cycle life. They store energy *via* electric double-layer capacitance or pseudocapacitance from rapid surface redox processes. In integrated energy systems, materials like GO, CNTs, or conducting polymers, which are utilized for harvesting moisture-induced charges, can also act as one of the electrodes in supercapacitors. GO films, which generate mobile ions from water vapor, can simultaneously serve as high-surface-area charge storage media. This dual functionality simplifies device architecture, diminishes system size, and facilitates autonomous self-charging energy storage.

Most implemented systems utilize solid-state or gel electrolytes, such as PVA- $\text{H}_3\text{PO}_4$  or ionic hydrogels, to maintain mechanical flexibility, ionic conductivity, and water retention.<sup>133,134</sup> Layouts generally follow sandwich or in-plane

architectures, with humidity-responsive electrodes that are aligned and enclosed for durability under ambient settings.

A recent study revealed a versatile moisture-powered supercapacitor (mp-SC) that utilizes moisture-induced ion diffusion from a polyelectrolyte generator and stores charge in GO-based electrodes, attaining an area capacitance of  $138.3 \text{ mF cm}^{-2}$  and maintaining stable voltage retention ( $\sim 96.6\%$ ) over 120 h. When connected in series, packs of 72 of these units produced 60 V in air, which directly powered commercial electronics. This demonstrated a practical, self-sustaining operation without the need for external charging sources.<sup>135</sup> Complementing this, a graphene-carbon black/PVC composite film was utilized to concurrently harvest energy from rain and store it through interfacial pseudocapacitance. This approach showed durable and repeatable charge-discharge behavior under continuous water exposure.<sup>136</sup> Furthermore, an MEG inspired by capacitors was developed using paired charged electrodes and a nanofiber film loaded with electrolytes, taking advantage of electric double-layer capacitor (EDLC) mechanisms. The device produced an output of 0.7 V and  $3 \mu\text{A}$  over 120 hours, operating well across a relative humidity range of 35–95%, underscoring the promise of capacitive topologies for improving the long-term stability of humidity-driven energy systems.<sup>137</sup>

Integrated devices like these showcase self-charging supercapacitor systems that collect moisture-generated ions and store them for external use, with fast charging, meaningful energy retention, and extended operational lifetimes. Integrated designs have also explored coupling moisture/light hybrid generators with storage elements. A light-moisture coupling power system successfully charged an energy storage capacitor, indicating the feasibility of hybrid humidity harvesting with on-board storage for autonomous micro-power applications.<sup>138</sup> However, challenges remain in improving the interface between harvesting and storage materials, reducing internal resistance, and keeping performance stable over time under changing moisture conditions.

### 4.2 Microbattery and hybrid storage systems

Microbatteries, including thin-film solid-state and flexible types, offer ideal energy density in tiny configurations, making them perfect candidates for integrated self-powered devices. Although their integration with humidity harvesters is still in the preliminary stages compared to supercapacitors, recent advances in functional materials have opened the door to novel hybrid architectures. Materials such as  $\text{MoS}_2$ , MXenes, and MOFs have significant promise for dual functionality owing to their elevated surface area, adjustable conductivity, and suitability for humid conditions. Although current research predominantly explores these materials either for energy storage or humidity sensing independently, their properties suggest that they could be engineered in future devices to serve as both harvesting and storage materials within compact hybrid platforms.<sup>139–143</sup>

In addition to storage-oriented hybrids, complementary multi-modal energy harvesting methods have also been investigated. The integration of moisture harvesting with light-





**Table 3** Summary of integrated humidity-driven energy harvesting and storage systems: materials, architectures, and key performance metrics<sup>a</sup>

Integration type	Energy storage	Harvesting material	Storage material	Architecture/design	Electrolyte	Performance	Application	Challenges	Ref
SC	GO-based SC	PDDA:PSS (polyelectrolyte)	GO/rGO	mp-SC, in-plane	PVA/LiCl (solid-state gel)	138.3 mF cm <sup>2</sup> ; 60 V from 72 units	Powering commercial electronics	Moisture variability, scale-up	119
SC	SC (Pseudocap.)	G-CB/PVC	G-CB/PVC	Interfacial pseudocapacitance under rain	0.6 M NaCl (rainwater)	Repeatable charge/discharge	Rain-powered remote systems	Environmental exposure	120
Capacitor-inspired MEG	EDLC	LiCl electrolyte-loaded PAN nanofiber film	Electrode-electrolyte interface (capacitor-inspired)	Capacitor-inspired paired electrode system	NaCl aqueous solution	0.7 V, 3 μA, stable for 120 h across 35–95% RH	Direct powering of respiration monitors, touch sensors, and small electronics	Maintaining long-term stability under fluctuating RH; scaling electrode/electrolyte integration	121
Conceptual/separate components*	Thin-film solid-state	MXenes, MoS <sub>2</sub> , MOFs (potential dual-functionality)	MXenes, MOFs (battery electrodes)	Emerging hybrid architectures; harvesting and storage materials currently used in separate roles	Solid-state/Ion-conducting gels (for energy storage only)	High energy density (e.g., >200 mA h g <sup>-1</sup> ), long cycle life (e.g., >1000 cycles); no moisture-induced generation data	Battery-powered wearable electronics, sensors, and IoT (storage side only)	No experimental dual role shown yet; lack of integrated moisture-harvesting function	122–135
Hybrid (MEG + TENG)	External capacitor	PVA/MXene-coated melamine foam (for MEG) + triboelectric layers (Cu/PFA film for TENG)	N/A	Layered hybrid device combining MEG and TENG in a deformable, stretchable form	Hygroscopic ionic hydrogel (PVA/LiCl) for MEG	MEG + TENG: 55 V, 102 μA and a high electric power of ~83 μW cm <sup>-2</sup> ; continuous powering of small electronics	Wearable electronics, self-powered sensors, deformation-adaptive devices	Complex architecture; matching impedance and output between MEG and TENG	136
Monolithic (conceptual/not yet realized for humidity-driven systems)**	SC	GO films or polyaniline-coated materials (conductive, hygroscopic)	Same as harvesting material (dual-function layer)	Single active layer or layered structure combining MEG and supercapacitor functions in one compact unit	Not reported (future work)	Not reported; anticipated high compactness, reduced footprint, and improved reliability	Self-powered electronics, IoT devices, wearable systems	Lack of demonstrated monolithic MEG-supercapacitor devices in literature; material compatibility optimization; balancing ion harvesting and charge storage efficiency; scalable fabrication methods	137–145

<sup>a</sup> \* MoS<sub>2</sub>, MXenes, and MOFs show promise for hybrid architectures, yet no experimental study has demonstrated their dual role as harvesting and storage materials in a single humidity-driven system. \*\* No experimental reports to date have demonstrated fully monolithic integration of humidity-driven generators with supercapacitors, highlighting a promising direction for compact and self-sustaining power systems. SC: supercapacitor. G-CB/PVC: graphene-carbon black/polyvinyl chloride. PDDA: polydiallyl dimethyl ammonium chloride. PSS: polystyrene sulfonic acid. EDLC: electrical double-layer capacitor. PVA: polyvinyl alcohol. mp: moisture-powered. MXenes: two-dimensional transition metal carbides, nitrides, or carbonitrides. MoS<sub>2</sub>: molybdenum disulfide. MOFs: metal-organic frameworks. PFA: perfluoroalkoxy.

responsive materials has been applied to improve hydrovoltaic performance when exposed to light. In one such system, a moisture-light harvesting electric generator constructed from hygroscopic polymers and light-responsive BiOBr nanosheets increased power output under simultaneous humidity and light exposure, demonstrating the efficacy of coupling water adsorption with light-induced charge dynamics for dual-modal environmental energy conversion.<sup>144</sup> In parallel, deformable hybrid energy harvesters incorporating MEGs and TENGs with MXene-coated foams and ionic hydrogels illustrate the practicality and performance benefits of multifunctional and hybrid platforms.<sup>145</sup>

Extending these concepts toward broader environmental adaptability, all-weather hybrid energy harvesters have been developed that integrate hydrovoltaic and photovoltaic conversion processes within a single platform. All-biobased hydrovoltaic-photovoltaic power generators allow the use of both ambient moisture and solar energy at the same time. This makes them more flexible and improves energy availability in different settings. Such systems illustrate viable strategies for coupling distinct harvesting mechanisms to achieve more continuous and reliable power generation.<sup>146</sup>

Hybrid systems, despite their potential, encounter significant limits, including the need for moisture-stable electrolytes, slower charging rates under ambient humidity, and the requirement to minimize internal resistance to ensure sustained long-term operation.

### 4.3 Design strategies for Co-integration

The integration of humidity harvesters and storage components is fundamentally dependent on the compatibility of materials and architectural design. Monolithic integration is an ambitious architectural goal, wherein a singular active material or layered structure simultaneously harvests moisture-induced ions and functions as an energy storage electrode, effectively merging the capabilities of moisture energy harvesting and supercapacitor technology into a unified compact unit. Substrates such as GO films or polyaniline-coated materials provide advantageous platforms for attaining dual functionality owing to their intrinsic conductivity, ion transport characteristics, and capacity to engage with ambient moisture.<sup>147–151</sup> Similar concepts have been realized in other energy domains, such as photosupercapacitors and MXene-based on-chip micro-supercapacitors, but the literature currently lacks any successful implementations of monolithic harvest-storage integration, specifically for humidity-driven systems.<sup>152,153</sup> This research gap offers a considerable opportunity for future advancement because the achievement of a genuine MEG-supercapacitor monolithic device will considerably simplify device architecture, decrease volume, and perhaps improve reliability in self-powered applications.

Layered architectures represent an alternative strategy that facilitates the independent optimization of harvesting and storage layers. This configuration consists of hydrophilic moisture-harvesting layers positioned above storage layers made of high surface area CC, conductive polymers, or ionic

hydrogels. This vertical or thin-film design enables precise modulation of humidity sensitivity and charge retention.<sup>135</sup>

Interdigitated electrode patterns are especially useful in planar designs. Inkjet, screen printing, or photolithography enable side-by-side harvesting and storage regions on a single substrate, eliminating complex wiring and facilitating transparent, lightweight, or flexible device formats. Interdigitated supercapacitors using double-layer active materials indicate potential in flexible hybrid platforms.<sup>154,155</sup>

Flexible and stretchable substrates, such as polydimethylsiloxane (PDMS), polyethylene terephthalate (PET), and thermoplastic polyurethane (TPU), have significantly enhanced integration possibilities. Hybrid platforms combining hygroscopic harvesting layers and stretchable storage modules are now viable for wearable electronics, soft robotics, and implantable devices.<sup>156,157</sup>

The selection of a co-integration strategy ultimately hinges on various factors, including power requirements, desired form factor, operating environment, and mechanical constraints. Progress in materials science and microfabrication is anticipated to produce more intricate integration schemes, facilitating compact, self-powered, and robust humidity energy systems.

To provide a comparative overview of current integration strategies between humidity-driven energy harvesters and storage systems, Table 3 summarizes recent advancements, including the types of energy storage used, materials employed, structural configurations, electrolytes, performance metrics, potential applications, and key integration challenges. This comparative table outlines the adaptability and constraints of current systems while highlighting essential design factors for future advancements.

### 4.4 Toward self-powered systems

The integration of humidity-driven energy harvesters with on-board storage represents an essential advancement in achieving self-powered electronic systems. Such systems can operate independently of external power sources, diminish maintenance requirements (e.g., battery replacement), and facilitate installation in remote or resource-limited environments.

Although most current prototypes demonstrate limited energy output and storage capacity, continued advancements in material design, multifunctional architectures, and energy management circuits are expected to enhance the feasibility of commercial applications. Future directions may encompass the use of smart packaging, bio-integrated energy systems, and adaptive harvesting circuits that responsively adjust to environmental stimuli to enhance both generation and storage.

Although current demonstrations remain at the proof-of-concept level, MEG-supercapacitor and MEG-battery hybrids represent a promising pathway toward self-powered systems, warranting further exploration of scalable integration strategies.

## 5. Applications, challenges, and concluding outlook

Humidity-driven energy harvesting technology shows great promise in addressing the increasing demand for self-powered







## Author contributions

Soheil Malekghasemi: conceptualization, investigation, methodology, writing – original draft. Serdar Abaci: writing – review & editing, supervision.

## Conflicts of interest

There are no conflicts of interest to declare.

## Data availability

This is a review article and does not report any new data. All data supporting the findings of this study are available in the cited references.

## References

- C. Jiang, X. Li, S. W. M. Lian, Y. Ying, J. S. Ho and J. Ping, *ACS Nano*, 2021, 9328–9354.
- X. Li, X. Zeng, J. Li, B. Li, Y. Chen and X. Zhang, *Friction*, 2024, 1655–1679.
- R. Yu, S. Feng, Q. Sun, H. Xu, Q. Jiang, J. Guo, B. Dai, D. Cui and K. Wang, *J. Nanobiotechnol.*, 2024, 497.
- B. Zhang, W. Xu, L. Peng, Y. Li, W. Zhang and Z. Wang, *Nat. Rev. Electr. Eng.*, 2024, 1, 218–233.
- M. R. Sarker, A. Riaz, M. S. H. Lipu, M. H. Md Saad, M. N. Ahmad, R. A. Kadir and J. L. Olazagoitia, *Heliyon*, 2024, e27778.
- G. Zhou, L. Huang, W. Li and Z. Zhu, *J. Sens.*, 2014, 1–20.
- A. Chakraborty, G. Lucarelli, J. Xu, Z. Skafi, S. Castro-Hermosa, A. B. Kaveramma, R. G. Balakrishna and T. M. Brown, *Nano Energy*, 2024, 109932.
- R. Singh, S. Dogra, S. Dixit, N. I. Vatin, R. Bhardwaj, A. K. Sundramoorthy, H. C. S. Perera, S. P. Patole, R. K. Mishra and S. Arya, *Hybrid Adv.*, 2024, 5, 100176.
- C. Callaty, C. Rodrigues and J. Ventura, *Nano Energy*, 2025, 110661.
- J. Tan, X. Wang, W. Chu, S. Fang, C. Zheng, M. Xue, X. Wang, T. Hu and W. Guo, *Adv. Mater.*, 2024, 2211165.
- L. Yang, L. Zhang and D. Sun, *ACS Appl. Mater. Interfaces*, 2022, 14, 53615–53626.
- T. Oksana and G. Dmytro, Earth's water distribution, *Clean Water and Sanitation*, 2021, pp. 1–14.
- L. Yang, D. K. Nandakumar, L. Miao, L. Suresh, D. Zhang, T. Xiong, J. V. Vaghasiya, K. C. Kwon and S. Ching Tan, *Joule*, 2020, 4, 176–188.
- Y. Komazaki, T. Nobeshima, H. Hiram, Y. Watanabe, K. Suemori and S. Uemura, *Adv. Energy Sustain. Res.*, 2025, 6, 2400342.
- H. G. Armstrong, *Dublin Philos. Mag. J. Sci.*, 1840, 17, 370–374.
- M. Faraday, *Philos. Trans. R. Soc. London*, 1843, 133, 17–32.
- M. Z. Bazant and T. M. Squires, *Phys. Rev. Lett.*, 2004, 92, 066101.
- L. Bocquet and E. Charlaix, *Chem. Soc. Rev.*, 2010, 39, 1073–1095.
- L. Jouniaux and C. Bordes, *Int. J. Geophys.*, 2012, 1–11.
- S. Ghosh, A. K. Sood and N. Kumar, *Science*, 2003, 299, 1042–1044.
- I. Jung, D. Dikin, S. Park, W. Cai, S. L. Mielke and R. S. Ruoff, *J. Phys. Chem. C*, 2008, 112, 20264–20268.
- F. Zhao, H. Cheng, Z. Zhang, L. Jiang and L. Qu, *Adv. Mater.*, 2015, 27, 4351–4357.
- D. W. Chang and J. B. Baek, *Nano Today*, 2017, 38–53.
- G. Xue, Y. Xu, T. Ding, J. Li, J. Yin, W. Fei, Y. Cao, J. Yu, L. Yuan, L. Gong, J. Chen, S. Deng, J. Zhou and W. Guo, *Nat. Nanotechnol.*, 2017, 12, 317–321.
- Z. Zhang, X. Li, J. Yin, Y. Xu, W. Fei, M. Xue, Q. Wang, J. Zhou and W. Guo, *Nat. Nanotechnol.*, 2018, 1109–1119.
- L. Yang, L. Zhang and D. Sun, *ACS Appl. Mater. Interfaces*, 2022, 14, 53615–53626.
- K. S. Moreira, D. Lermen, L. P. Dos Santos, F. Galembeck and T. A. L. Burgo, *Energy Environ. Sci.*, 2021, 14, 353–358.
- J. Chi, C. Liu, L. Che, D. Li, K. Fan, Q. Li, W. Yang, L. Dong, G. Wang and Z. L. Wang, *Adv. Sci.*, 2022, 9, 2201586.
- Z. Sun, X. Wen, L. Wang, D. Ji, X. Qin, J. Yu and S. Ramakrishna, *eScience*, 2022, 32–46.
- D. Shen, W. W. Duley, P. Peng, M. Xiao, J. Feng, L. Liu, G. Zou and Y. N. Zhou, *Adv. Mater.*, 2020, 2003722.
- J. Yin, N. Liu, P. Jia, Z. Ren, Q. Zhang, W. Lu, Q. Yao, M. Deng and Y. Gao, *SusMat*, 2023, 3, 859–876.
- W. Duan, Z. Sun, X. Jiang, S. Tang and X. Wang, *Nano Energy*, 2025, 110516.
- H. Yan, R. Qi, Z. Liu, H. Wang, C. Dong and L. zhi Zhang, *Device*, 2024, 3, 100568.
- K. Calautit, D. S. N. M. Nasir and B. R. Hughes, *Renew. Sustain. Energy Rev.*, 2021, 147, 111230.
- H. Liu, H. Fu, L. Sun, C. Lee and E. M. Yeatman, *Renewable Sustainable Energy Rev.*, 2021, 110473.
- L. Xu, H. Zhai, X. Chen, Y. Liu, M. Wang, Z. Liu, M. Umar, C. Ji, Z. Chen, L. Jin, Z. Liu, Q. Song, P. Yue, Y. Li and T. T. Ye, *Chem. Eng. J.*, 2021, 412, 128639.
- D. Maity and M. Fussenegger, *Adv. Sci.*, 2023, 10, 2300750.
- H. Shen, K. Xu, Y. Duan, P. Wu, Z. Qian, Y. Chen, Y. Luo, C. Liu, Y. Li, J. Cui and D. Liu, *Adv. Sci.*, 2023, 10, 2206483.
- X. Zhang, J. Liang, K. Ahmad, Z. Almutairi and C. Wan, *Device*, 2024, 2, 100316.
- G. Zan, W. Jiang, H. Y. Kim, K. Zhao, S. Li, K. Lee, J. Jang, G. Kim, E. A. Shin, W. Kim, J. W. Oh, Y. Kim, J. W. Park, T. Kim, S. Lee, J. H. Oh, J. Shin, H. J. Kim and C. Park, *Nat. Commun.*, 2024, 15, 1–13.
- H. Yan, R. Qi, Z. Liu, H. Wang, C. Dong and L. zhi Zhang, *Device*, 2024, 3, 100568.
- Y. Cheng, T. Zhu, Q. He, F. Wen, Y. Cheng, J. Huang, Y. Lai and H. Li, *Adv. Funct. Mater.*, 2025, 2500186.
- Y. Lee, M. Lee, J. Lee, H. W. Jang and J. S. Jang, *Exploration*, 2025, 70007.
- C. Xu, C. Fu, Z. Jiang, T. Yang and M. Xin, *ACS Appl. Nano Mater.*, 2023, 6, 5930–5938.
- L. Yang, L. Zhang and D. Sun, *ACS Appl. Mater. Interfaces*, 2022, 14, 53615–53626.
- D. Thakur, H. J. Youn and J. Hyun, *Cellulose*, 2025, 32, 3285–3298.



- 47 C. Fu, J. Zhou, X. Lu, H. Feng, Y. Zhang, K. Shang, Z. Jiang, Y. Yao, Q. C. He and T. Yang, *Adv. Sci.*, 2024, **11**, 2305530.
- 48 Y. Huang, H. Cheng, C. Yang, P. Zhang, Q. Liao, H. Yao, G. Shi and L. Qu, *Nat. Commun.*, 2018, **9**, 1–8.
- 49 Z. Feng, G. Hu, R. Zhu, S. Zhang, C. Liu, P. Guan, M. Li, T. Wan, H. Xu and D. Chu, *ACS Appl. Nano Mater.*, 2022, **5**, 12224–12244.
- 50 J. Chen, X. Zhang, M. Cheng, Q. Li, S. Zhao, M. Zhang, Q. Fu and H. Deng, *Mater. Horizons*, 2025, **12**, 2309–2318.
- 51 X. Qi, T. Miao, C. Chi, G. Zhang, C. Zhang, Y. Du, M. An, W. G. Ma and X. Zhang, *Nano Energy*, 2020, **77**, 105096.
- 52 C. S. Kushwaha, P. Singh, S. K. Shukla and G. C. Dubey, *J. Electron. Mater.*, 2023, **52**, 1785–1793.
- 53 Y. Yang, J. Wang, Z. Wang, C. Shao, Y. Han, Y. Wang, X. Liu, X. Sun, L. Wang, Y. Li, Q. Guo, W. Wu, N. Chen and L. Qu, *Nano-Micro Lett.*, 2024, **16**, 1–16.
- 54 P. Li, Y. Hu, H. Wang, T. He, H. Cheng and L. Qu, *Nat. Commun.*, 2025, **16**, 6600.
- 55 C. Yang, Y. Huang, H. Cheng, L. Jiang and L. Qu, *Adv. Mater.*, 2019, **31**, 1805705.
- 56 W. Xue, Z. Zhao, S. Zhang, Y. Li, X. Wang and J. Qiu, *ACS Appl. Mater. Interfaces*, 2024, **16**, 2825–2835.
- 57 X. Li, C. Shen, Q. Wang, C. M. Luk, B. Li, J. Yin, S. P. Lau and W. Guo, *Nano Energy*, 2017, **32**, 125–129.
- 58 X. Guo, D. Kuang, Z. Zhu, Y. Ding, L. Ge, Z. Wu, B. Du, C. Liang, G. Meng and Y. He, *ACS Appl. Nano Mater.*, 2021, **4**, 11159–11167.
- 59 E. Farahani and R. Mohammadpour, *Sci. Rep.*, 2020, **10**, 1–8.
- 60 R. Malik, V. K. Tomer, V. Chaudhary, M. S. Dahiya, A. Sharma, S. P. Nehra, S. Duhan and K. Kailasam, *J. Mater. Chem. A*, 2017, **5**, 14134–14143.
- 61 G. Ren, Q. Hu, J. Ye, X. Liu, S. Zhou and Z. He, *Chem. Eng. J.*, 2022, **441**, 135921.
- 62 Q. Hu, G. Ren, J. Ye, B. Zhang, C. Rensing and S. Zhou, *Chem. Eng. J.*, 2023, **452**, 139169.
- 63 P. Guo, B. Tian, J. Liang, X. Yang, G. Tang, Q. Li, Q. Liu, K. Zheng, X. Chen and W. Wu, *Adv. Mater.*, 2023, **35**, 2304420.
- 64 S. Andrić, T. Tomašević-Ilić, M. V. Bošković, M. Sarajlić, D. Vasiljević-Radović, M. M. Smiljanić and M. Spasenović, *Nanotechnology*, 2021, **32**, 025505.
- 65 Y. Dou, C. Tang and Y. Lu, *Langmuir*, 2023, **39**, 17436–17445.
- 66 F. Gao, J. Tu, J. Qu, J. Ge, Q. Yin, Y. Zang, W. Zhong and Z. Jiao, *J. Colloid Interface Sci.*, 2024, **663**, 251–261.
- 67 X. Zhou, W. Zhang, C. Zhang, Y. Tan, J. Guo, Z. Sun and X. Deng, *ACS Appl. Mater. Interfaces*, 2020, **12**, 11232–11239.
- 68 T. Tabrizizadeh, J. Wang, R. Kumar, S. Chaurasia, K. Stampleskoskie and G. Liu, *ACS Appl. Mater. Interfaces*, 2021, **13**, 50900–50910.
- 69 Z. Gong, A. Suwardi and J. Cao, *Adv. Funct. Mater.*, 2025, 2423371.
- 70 J. Fang, X. Zhang, P. Duan, Z. Jiang, X. Lu, C. Fu, Y. Zhang, Y. Yao, K. Shang, J. Qin, Y. Liu and T. Yang, *Mater. Horizons*, 2023, **11**, 1261–1271.
- 71 Y. Liu, B. Xiao, Q. Wei, Z. Yuan, W. Song, L. Zhou and W. Ge, *RSC Adv.*, 2024, **14**, 18832–18837.
- 72 A. Yaroshchuk, *Adv. Colloid Interface Sci.*, 2022, 102708.
- 73 V. U. Somkuwar, H. Garg, S. K. Maurya and B. Kumar, *ACS Appl. Electron. Mater.*, 2024, **6**, 931–939.
- 74 A. Repoulias, M. Ertekin, S. F. Galata, J. Pesez, C. Anicaux, S. Vassiliadis and A. Marmarali, *Energy Technol.*, 2023, **11**, 2201433.
- 75 J. Wang, Z. Xia, H. Yao, Q. Zhang and H. Yang, *ACS Appl. Mater. Interfaces*, 2023, **15**, 47208–47220.
- 76 F. Ejehi, R. Mohammadpour, E. Asadian, S. Fardindoost and P. Sasanpour, *Microchim. Acta*, 2021, **188**, 1–13.
- 77 I. S. M. Jimidar, W. Kwiecinski, G. Roozendaal, E. S. Kooij, H. J. G. E. Gardeniers, G. Desmet and K. Sotthewes, *ACS Appl. Mater. Interfaces*, 2023, **15**, 42004–42014.
- 78 J. Zhang, C. Boyer and Y. X. Zhang, *Small*, 2024, 2401846.
- 79 L. Liu, L. Zhou, C. Zhang, Z. Zhao, S. Li, X. Li, X. Yin, J. Wang and Z. L. Wang, *J. Mater. Chem. A*, 2021, **9**, 21357–21365.
- 80 J. Oh, M. Kang, J. Park, T. Y. Kim, K. Park and J. Seo, *Adv. Electron. Mater.*, 2024, **10**, 2400013.
- 81 J. Zhang, X. Zhou, M. Wu, L. Zhu, Z. Ming, W. Li, Y. Xia, H. Liu, Z. Zhou, T. Zhang, M. Fan, J. Yu and J. Xiong, *Chem. Eng. J.*, 2025, **521**, 166584.
- 82 Q. Chen, J. Zhao and H. Cheng, *Front. Energy Res.*, 2021, **9**, 738142.
- 83 L. Chang, D. Wang, A. Jiang and Y. Hu, *ChemPlusChem*, 2022, e202100437.
- 84 F. Chen, S. Zhang, P. Guan, Y. Xu, T. Wan, C. H. Lin, M. Li, C. Wang and D. Chu, *Small*, 2023, **20**, 2304572.
- 85 P. Faramarzi, B. Kim, J. B. You and S. H. Jeong, *J. Mater. Chem. C*, 2023, **11**, 2206–2216.
- 86 B. Saikia, M. Dey, P. Garg, R. Gogoi, R. Manik and K. Raidongia, *Chem. Eng. J.*, 2024, **497**, 154840.
- 87 W. Duan, Z. Sun, X. Jiang, S. Tang and X. Wang, *Nano Energy*, 2025, 110516.
- 88 X. Wang, L. Wang, W. Xiu, X. Yang, Y. Yang and X. Li, *ACS Appl. Nano Mater.*, 2024, **7**, 7327–7336.
- 89 Q. Lyu, B. Peng, Z. Xie, S. Du, L. Zhang and J. Zhu, *ACS Appl. Mater. Interfaces*, 2020, **12**, 57373–57381.
- 90 B. C. Kang, S. J. Park, H. J. Choi and T. J. Ha, *Nano Energy*, 2022, **104**, 107890.
- 91 G. Ma, W. Li, X. Zhou, X. Wang, M. Cao, W. Ma, J. Wang, H. Yu, S. Li and Y. Chen, *ACS Appl. Polym. Mater.*, 2024, **6**, 7066–7076.
- 92 J. Qian, R. Tan, M. Feng, W. Shen, D. Lv and W. Song, *Chemosensors*, 2024, 230.
- 93 S. Li, S. Hernandez and N. Salazar, *Sustainability*, 2023, 848.
- 94 H. Zhang, M. Sun, Q. Meng, H. Li and Y. Tian, *Soft Sci*, 2025, **5**, 23.
- 95 M. Shi, Y. Yang, Y. Han, J. Wang, Y. Wang, D. Li, J. Lv, W. Wu, Z. Wang, X. Wei and N. Chen, *Adv. Energy Mater.*, 2024, **14**, 2303815.
- 96 H. Zhang, N. He, B. Wang, B. Ding, B. Jiang, D. Tang and L. Li, *Adv. Mater.*, 2023, **35**, 2300398.
- 97 H. Yan, R. Qi, Z. Liu, H. Wang, C. Dong and L. zhi Zhang, *Devic*, 2025, **3**, 100568.



- 98 S. Yang, X. Tao, W. Chen, J. Mao, H. Luo, S. Lin, L. Zhang and J. Hao, *Adv. Mater.*, 2022, **34**, 2200693.
- 99 W. Ying, Z. Huang, Z. Liu, J. Liu, N. Pan, A. Jazzar, J. Zhang, H. Zhang, X. He, R. Wang and J. Wang, *Energy Environ. Sci.*, 2025, **18**, 9457–9467.
- 100 W. Zang, W. Wang, D. Zhu, L. Xing and X. Xue, *RSC Adv.*, 2014, **4**, 56211–56215.
- 101 W. Zang, P. Li, Y. Fu, L. Xing and X. Xue, *RSC Adv.*, 2015, **5**, 84343–84349.
- 102 B. Yu, Y. Fu, P. Wang, Y. Zhao, L. Xing and X. Xue, *Phys. Chem. Chem. Phys.*, 2015, **17**, 10856–10860.
- 103 Y. A. Çetin, L. Escorihuela, B. Martorell and F. Serratos, *ACS Omega*, 2025, **10**, 4449–4457.
- 104 G. Ge, N. Ke, H. Ma, J. Ding, W. Zhang and X. Fan, *Nanoscale*, 2024, **16**, 17804–17816.
- 105 Z. Cui, C. Wang, X. Liu, L. Wang and L. J. Wang, *Langmuir*, 2024, **40**, 16361–16366.
- 106 D. Wang, D. Zhang, P. Li, Z. Yang, Q. Mi and L. Yu, *Nano-Micro Lett.*, 2021, **13**, 1–13.
- 107 J. C. Feng, S. X. Li, Z. P. Zhang, Y. An, Q. S. Gao, Z. Sun and H. Xia, *Nano Energy*, 2024, **119**, 109103.
- 108 P. Li, Y. Hu, W. He, B. Lu, H. Wang, H. Cheng and L. Qu, *Nat. Commun.*, 2023, **14**, 5702.
- 109 C. Zheng, S. Fang, W. Chu, J. Tan, B. Tian, X. Jiang and W. Guo, *Nano Res.*, 2023, **16**, 11320–11325.
- 110 H. Yan and R. Qi, *ACS Appl. Electron. Mater.*, 2023, **5**, 5809–5813.
- 111 X. Wang, Y. Lin, S. Jiao and X. Liu, *Chem. Commun.*, 2025, **61**(85), 16572–16575.
- 112 J. Mo, X. Wang, X. Lin, X. Feng, C. Qiu, S. Tao, P. Chen, K. Zhu and H. Qi, *Chem. Eng. J.*, 2024, **491**, 152055.
- 113 M. Zhang, Y. Duan, T. Chen, J. Qi, T. Xu, H. Du and C. Si, *Ind. Crops Prod.*, 2023, **203**, 117174.
- 114 M. M. Islam, *Sustainable Energy Fuels*, 2024, 1823–1871.
- 115 Y. Ding, L. Deng, X. X. Liu, L. Wang, Y. Meng, M. Ouyang, F. Chen, Z. X. Huang and T. Kuang, *Chem. Eng. J.*, 2025, 164101.
- 116 L. Lan, J. Ping, J. Xiong and Y. Ying, *Adv. Sci.*, 2022, 2200560.
- 117 M. S. Dennison, K. J. S., A. Samraj, O. S. Zaroog, T. Wanazusi, A. M. M. and N. Rajamani, *Discover Mater.*, 2025, 182.
- 118 W. Zhao, Q. Li, Q. Wang, Z. Li, J. Liang and W. Wu, *Sens. Actuators, B*, 2025, **440**, 137868.
- 119 Y. Yang, G. Su, Q. Li, Z. Zhu, S. Liu, B. Zhuo, X. Li, P. Ti and Q. Yuan, *RSC Adv.*, 2021, **11**, 1543–1552.
- 120 L. Wang, M. Xia, L. Li, Y. Wu, Q. Cheng, J. Xu, S. He, K. Liu and D. Wang, *J. Colloid Interface Sci.*, 2024, **674**, 1019–1024.
- 121 T. Delipinar, A. Shafique, M. S. Gohar and M. K. Yapici, *ACS Omega*, 2021, 8744–8753.
- 122 X. Li, Y. Guo, J. Meng, X. Li, M. Li and D. Gao, *Langmuir*, 2022, **38**, 8232–8240.
- 123 C. Tang, H. Wang, Y. Dou and P. Lai, *ACS Omega*, 2024, 2025.
- 124 S. Wang, G. Li, J. Wen, J. Feng, H. Zhang and Y. Tian, *Materials*, 2025, **18**(12), 2766.
- 125 Y. Zu, Z. Duan, Z. Yuan, Y. Jiang and H. Tai, *J. Mater. Chem. A*, 2024, 27157–27179.
- 126 V. S. Reddy, Y. Tian, C. Zhang, Z. Ye, K. Roy, A. Chinnappan, S. Ramakrishna, W. Liu and R. Ghosh, *Polymers*, 2021, 3746.
- 127 R. Wei, H. Li, Z. Chen, Q. Hua, G. Shen and K. Jiang, *npj Flexible Electron.*, 2024, 83.
- 128 Z. Sun, X. Wen, J. Kim, K. Zhao, Q. Zhou, M. Mahato, V. H. Nguyen, Y. Yang, L. Wang and I. K. Oh, *Adv. Funct. Mater.*, 2025, e18814.
- 129 W. B. Han, S. W. Hwang and W. H. Yeo, *Flexible Printed Electron.*, 2024, 033001.
- 130 G. Bai, J. Li, T. Lan, T. Gao, A. El-Shaer, B. Shao and B. Sun, *Adv. Mater.*, 2025, e18509.
- 131 Y. Huang, Z. Zeng, T. Liang, J. Li, Z. Liao, J. Li and T. Yang, *Sens. Actuators, B*, 2023, **396**, 134517.
- 132 S. Fang, Y. Huang, S. Dang, K. Hazazi, Y. Cao, J. Wang, P. Wu, S. De Wolf, H. Qasem and Q. Gan, *Energy Environ. Sci.*, 2026, DOI: [10.1039/d5ee05530j](https://doi.org/10.1039/d5ee05530j).
- 133 S. Alipoori, M. M. Torkzadeh, S. Mazinani, S. H. Aboutalebi and F. Sharif, *SN Appl. Sci.*, 2021, **3**, 1–13.
- 134 S. Akbulut, M. Yilmaz, S. Raina, S. H. Hsu and W. P. Kang, *Diam. Relat. Mater.*, 2017, **74**, 222–228.
- 135 L. Wang, H. Wang, C. Wu, J. Bai, T. He, Y. Li, H. Cheng and L. Qu, *Nat. Commun.*, 2024, **15**, 1–9.
- 136 Y. Zheng, H. Zheng, Y. Yue, L. Lu, Y. Wang and Q. Tang, *Energy Adv.*, 2024, **3**, 2929–2938.
- 137 Z. Sun, X. Wen, L. Wang, J. Yu and X. Qin, *Energy Environ. Sci.*, 2022, **15**, 4584–4591.
- 138 C. Xu, X. Zhang, J. Fang, Y. Yao, Y. Zhang, X. Lu, T. Yang and M. Xin, *ACS Omega*, 2024, **9**, 42602–42611.
- 139 Y. Wang, P. Yuan, Z. Xu, X. X. Liu, S. Feng, M. Cao, C. Cao, X. Wang, L. Pan and Z. M. Sun, *Chinese Chem. Lett.*, 2024, **35**, 108776.
- 140 Z. Li, Z. Long, H. Dai, Z. Yan, K. Liu, H. Qiao, K. Wang and W. Li, *J. Power Sources*, 2024, **606**, 234586.
- 141 W. Waheed, S. Anwer, M. U. Khan, M. Sajjad and A. Alazzam, *Chem. Eng. J.*, 2024, **480**, 147981.
- 142 H. Xu, S. Liu, Z. Li, F. Ding, W. Wang, K. Song, T. Liu and L. Hu, *J. Mater. Sci. Technol.*, 2025, **223**, 104–113.
- 143 N. M. Pereira, N. P. Rezende, T. H. R. Cunha, A. P. M. Barboza, G. G. Silva, D. Lippross, B. R. A. Neves, H. Chacham, A. S. Ferlauto and R. G. Lacerda, *ACS Omega*, 2022, **7**, 9388–9396.
- 144 Z. Lu, H. Zhu, D. Wang, M. Ma, J. Wang, X. Zhong and F. Wang, *Adv. Mater.*, 2025, e15241.
- 145 G. Kim, J. W. Lee, K. Zhao, T. Kim, W. Kim, J. W. Oh, K. Lee, J. Jang, G. Zan, J. W. Park, S. Lee, Y. Kim, W. Jiang, S. Li and C. Park, *Energy Environ. Sci.*, 2023, **17**, 134–148.
- 146 G. Ren, Q. Hu, J. Ye, A. Hu, J. Lü and S. Zhou, *Research*, 2022, DOI: [10.34133/2022/9873203](https://doi.org/10.34133/2022/9873203).
- 147 Q. Yang, Q. Wei and Y. Fang, *Sustain. Chem. Energy Mater.*, 2025, **1**, 100006.
- 148 F. Fenniche, Y. Khane, D. Aouf, S. Albukhaty, F. Z. Nouasria, M. Chouireb, N. Harfouche, A. Henni, G. M. Sulaiman, M. S. Jabir, H. A. Mohammed and M. M. Abomughaid, *Sci. Rep.*, 2024, **14**, 1–14.



- 149 Y. Ma, Y. He, C. Hao, X. Li, L. Li, Y. Zhao, Y. Zhang and W. Zhang, *J. Colloid Interface Sci.*, 2025, **696**, 137860.
- 150 M. Khairy, M. A. Mousa, R. Kamal and M. Sameeh, *J. Text. Inst.*, 2025, 1–20.
- 151 D. Y. Imali, E. C. J. Perera, M. N. Kaumal and D. P. Dissanayake, *RSC Adv.*, 2023, **13**, 6396–6411.
- 152 Y. Gogotsi, *Natl. Sci. Rev.*, 2023, **10**(3), nwad020.
- 153 J. Kim, S. M. Lee, Y. H. Hwang, S. Lee, B. Park, J. H. Jang and K. Lee, *J. Mater. Chem. A*, 2017, **5**, 1906–1912.
- 154 A. Paul, N. C. Murmu and T. Kuila, *EcoEnergy*, 2025, **3**, 3–24.
- 155 A. He, J. He, L. Cao, J. Chen, B. Cheng, R. Ma, Y. Ding, G. Yang and F. Yi, *Adv. Mater. Technol.*, 2024, 2301931.
- 156 X. Zhang, J. Liang, K. Ahmad, Z. Almutairi and C. Wan, *Device*, 2024, **2**, 100316.
- 157 M. Cheng, K. Tian, T. Qin, Q. Li, H. Deng and Q. Fu, *SusMat*, 2024, **4**, e204.
- 158 A. Beniwal, G. Khandelwal, R. Mukherjee, D. M. Mulvihill and C. Li, *ACS Appl. Bio Mater.*, 2024, **7**, 4772–4784.
- 159 Y. Pang, J. Jian, T. Tu, Z. Yang, J. Ling, Y. Li, X. Wang, Y. Qiao, H. Tian, Y. Yang and T. L. Ren, *Biosens. Bioelectron.*, 2018, **116**, 123–129.
- 160 S. A. Khan, M. M. Rehman, S. Iqbal, M. M. Baig, S. G. Lee and W. Y. Kim, *Chem. Eng. J.*, 2024, **495**, 153376.
- 161 N. I. Hossain, K. Saha, A. Sharma and S. Sonkusale, *arXiv Prepr. arXiv*, 2025, 2509.14240.
- 162 Y. Guo, Q. Gong, D. Liu and G. Nie, *Chem. Eng. J.*, 2025, **507**, 160572.
- 163 H. Ma, J. Ding, Z. Zhang, Q. Gao, Q. Liu, G. Wang, W. Zhang and X. Fan, *IEEE Sens. J.*, 2024, **24**, 20289–20311.
- 164 S. Zhang, Z. He, W. Zhao, C. Liu, S. Zhou, O. O. Ibrahim, C. Wang and Q. Wang, *Nanomaterials*, 2024, 857.
- 165 J. Park, S. M. Chang, J. Shin, I. W. Oh, D. G. Lee, H. S. Kim, H. Kang, Y. S. Park, S. Hur, C. Y. Kang, J. M. Baik, J. S. Jang and H. C. Song, *Adv. Energy Mater.*, 2023, **13**, 2300530.
- 166 C. Xu, X. Zhang, J. Fang, Y. Yao, Y. Zhang, X. Lu, T. Yang and M. Xin, *ACS Omega*, 2024, **9**, 42602–42611.
- 167 J. Tan, X. Wang, W. Chu, S. Fang, C. Zheng, M. Xue, X. Wang, T. Hu and W. Guo, *Adv. Mater.*, 2024, 2211165.
- 168 J. C. Feng, S. X. Li, Z. P. Zhang, Y. An, Q. S. Gao, Z. Sun and H. Xia, *Nano Energy*, 2024, **119**, 109103.
- 169 D. Thakur, H. J. Youn and J. Hyun, *Cellulose*, 2025, **32**, 3285–3298.
- 170 K. Zhao, J. W. Lee, Z. G. Yu, W. Jiang, J. W. Oh, G. Kim, H. Han, Y. Kim, K. Lee, S. Lee, H. Y. Kim, T. Kim, C. E. Lee, H. Lee, J. Jang, J. W. Park, Y. W. Zhang and C. Park, *ACS Nano*, 2023, **17**, 5472–5485.
- 171 S. Chen, H. Xia and Q. Q. Ni, *Carbon N. Y.*, 2022, **194**, 104–113.
- 172 Y. Li, S. Tian, X. Chen, Y. Liao, F. Jiang, J. Ye, Y. He, Y. Gui, Z. Lian, G. Liu, J. Dai, L. Li, J. Chen, S. Liu, R. Zhu, Y. Lu and M. Gao, *J. Mater. Chem. A*, 2024, **12**, 33039–33052.

